Mathematics Letters
2025; 11(1): 10-31
http://www.sciencepublishinggroup.com/j/ml
doi: 10.11648/j.ml.20251101.12
ISSN: 2575-503X (Print); ISSN: 2575-5056 (Online)

A Circular Spatial-diffusion Mathematical Model to Analysis Hopf-Turing Bifurcation in Plankton Population Under the Toxin Control Variation in 2D

Hamidou Ouedraogo[1, *], Wendkouni Ouedraogo[2], Desire Ouedraogo[1], Boureima Sangare[2]

[1]Laboratory of Mathematics, Informatics (LaMIA), University Joseph Ki-Zerbo, Ouagadougou, Burkina Faso
[2]Laboratory of Mathematics, Informatics and Applications (LaMIA), Nazi Boni University, Bobo Dioulasso, Burkina Faso

Email address:

ameldo16@yahoo.fr (Hamidou Ouedraogo), wendkounio@yahoo.fr (Wendkouni Ouedraogo), desiweder@yahoo.fr (Desire Ouedraogo), mazou1979@yahoo.fr (Boureima Sangare)
*Corresponding author

To cite this article:

Hamidou Ouedraogo, Wendkouni Ouedraogo, Desire Ouedraogo, Boureima Sangare. (2025). A Circular Spatial-diffusion Mathematical Model to Analysis Hopf-Turing Bifurcation in Plankton Population Under the Toxin Control Variation in 2D. *Mathematics Letters, 11*(1), 10-31. https://doi.org/10.11648/j.ml.20251101.12

Received: 23 February 2025; **Accepted:** 6 March 2025; **Published:** 24 March 2025

Abstract: In a mathematical model of a system with two reaction-diffusion equations with Neumann-Dirichlet boundary conditions, we formulated zooplankton-phytoplankton in the aquatic environment on the circular domain. The attention has been focused on the toxin producing role of the space in explaining heterogeneity, the distribution of the species and the influence of the spatial structure on their abundance. The key idea of the model formulation is based on a nonlinear equations systems version with Holling II functional response. We base our mathematical analysis on the search for local and global solution with spatial diffusion. We present some mathematical results concerning the solution existence, the stability of the model equilibria. We have obtained important mathematical results for model equilibria stability at long time. Under certain mathematical conditions, the model without diffusion is locally asymptotically stable. Mathematical analysis also shows that the Hopf bifurcation breaks the time symmetry of the system and leads to uniform oscillations in space and periodic oscillations. The Turing bifurcation breaks the space symmetry and leads to the formation of stationary patterns in time and oscillatory patterns in space. A series of structured numerical simulations highlighted the formation of patterns and allowed to identify critical threshold of toxin released by phytoplankton leading to phytoplankton blooms.

Keywords: Cicular Domain, Phytoplankton-zooplankton, Toxin Parameter, Diffusion Coefficients, Global Stability, Dirichlet Boundary, Bifurcation Analysis, Pattern Formation

1. Introduction

Spatial or spatio-temporal heterogeneities are a characteristic of many ecological and epidemiological systems and have profound effects on invasion dynamics, population growth and persistence [2, 5]. These heterogeneities are determining factors in the self-organization of the system studied. The identification of factors allowing the transition from a stable homogeneous state to the emergence of spatial or spatio-temporal patterns is a question of great importance in the study of biological processes or in understanding the evolution of ecosystems. In the fisheries ecosystem, the majority of aquatic life is based on plankton. In particular, phytoplankton, the plant component of plankton, occupies the first trophic level. The fluctuations of its abundance determine the production of all marine biological production. Phytoplankton is normally present in these waters at low concentrations but can proliferate to form dense concentrations of cells on the water surfaces called “blooms” which correspond to an immense production of the toxin by the phytoplankton species. This strong diffusion of phytoplankton containing toxin greatly influences the spatial distribution of populations in the fish ecosystem. Phytoplankton is consumed by zooplankton, the animal component of plankton, which

provides food for fish and other aquatic animals [5, 11].

The need for a more in-depth understanding of the diffusion of planktonic organisms is important because their activities have implications on the ecosystem as a whole and ultimately affect human activities such as fishing and economic losses due to poor water quality. However, many biological factors including predation mode, inter-species competition, mutualism, etc., influence the spatial diffusion of these species, sometimes leading to instability in the marine environment. Also, the lack of control of the mechanism of toxin release by phytoplankton in the aquatic environment remains an open question for several decades. It is in this perspective that new reaction-diffusion models are necessary to study the spatial heterogeneity of the dynamics of these two species in a specific area and to try to explain the mechanism of toxin release by phytoplankton in the aquatic environment [2, 3].

A significant number of authors have drawn attention to a global increase in harmful phytoplankton blooms in recent decades through mostly predator-prey models, [1, 15]. Going through the very important role played by chaotic dynamics in reaction-diffusion models, the authors first show the mode of formation of spatial patterns through the different instability in the aquatic environment. So said, The interaction of the dynamics of a continuous model of two species has also been explored in the literature, [5, 10]. In these models, we observe an approach focused on the existence of stable equilibrium and sometimes which becomes unstable by presenting the limit cycle. We also observe a model of three species of the dynamics of the complex system, [10, 15]. These mathematical equations present a dissipative dynamic system whose graphical representations in space combine chaos, the limit cycle, the stable focus. The scientific results proposed in the literature of the last two years suggest that the very complex dynamics of food chain models with three or more species can occur in their ecosystems. These same results are observed in multi-species network models, [1, 5, 9]. According to May [8], the results still proposed in the literature, it appears that it is essential to understand the marine ecosystem without a proper study of nonlinear systems in this environment. Although the literature presents some results on chaos, there are fewer practical examples in scientific laboratories or in the field. Therefore, there is less evidence for explaining chaos so far. The reference [8], explains better why the natural terrestrial ecosystem does not manage to explain well the dynamics of systems possessing chaos. This is really surprising because the characteristics such as large dimensions, non-linearity, etc. of ecological models seem sufficient to better explore the dynamics of chaos in systems. Many scientific results have particularly ruled on the dynamics of non-linear and chaotic systems of natural populations [13, 14]. As a result, the focus is on the dynamics of aquatic systems when it comes to the concrete explanation of the systems responsible for chaos. In recent years, several recent studies have highlighted the usefulness of systems involving chaos in reaction diffusion models, [3, 13]. It emerged that two- or three-dimensional models would have characteristics of chaos attractors in most natural food chains. The complexity in this understanding lies in the instability of natural systems, their possibilities of rapidly passing from one state to another, even from chaos to order or from order to chaos. Plankton is considered the basis of the aquatic ecosystem because it plays a crucial role in the food chain and the production of food. Phytoplankton, which is at the origin of the production of the toxin, can sometimes be responsible for many changes of stable and unstable states in the aquatic environment. It is well known from the literature the role that phytoplankton plays in reducing the grazing pressure of this species by animal plankton, zooplankton, even fish, crustaceans and molluscs, [4]. This last toxic substance constitutes the stabilizer of the food chain in the aquatic environment according to some results examined in the field and by laboratories, [10]. It is most often observed that environments with high concentrations of phytoplankton organisms are avoided by zooplankton and fish. This finding of exclusion is mentioned in the work cited in [7, 12]. In the reference [12], the author has better explained the efficiency parameter in controlling aquatic diet. In the article entitled ”Nonlinear dynamics of a toxin-phytoplankton-zooplankton system with self-diffusion and cross-diffusion”, Pengfei Wang et al formulate and study the effect of self-diffusion and cross-diffusion on the system on the dynamics of the zooplankton-phytoplankton model in the aquatic environment. These authors add that the analysis of the cross-diffusion of said pairs of populations can play an important role in the formation of the spatial patterns of the models [15]. The complex dynamics model was set up to study the instability induced by a prey-predator system with cross-diffusion. Ecologically, the cross-diffusion of a model stipulates the counter-transport mechanism and further explains the influence of the self-defense set up by the prey against its predator. This mechanism is different from self-diffusion and it is possible to observe negative and positive cross-diffusion [9, 13]. For some time, the impact of the toxin produced by phytoplankton has been the subject of several related researches in models of the phytoplankton-zooplankton forms to study the dynamic behaviors of toxic phytoplankton. Chattopadhyay et al, [5] based on observations of natural phonomena and existing mathematical models that the toxin released by phytoplankton has the ability to terminate blooms of plankton species by decreasing the grazing pressure of zooplankton and can serve as a biological controller in the aquatic ecosystem. At the same time, by formulating and conducting an analysis of a phytoplankton-zooplankton interaction model under three forms of toxicant release, respectively: (a) a Holling II type, (b) a gamma distribution and (c) a discrete type, Chattopadhyay et al. [5, 9] confirmed again that the toxin produced by phytoplankton species can play an important role in terminating blooms.

Pal et al in the bibliography [12] obtained a similar result by considering a phytoplankton-zooplankton nutrient model. They showed that the toxin concentration exceeding a threshold level dampens the phytoplankton-zooplankton population oscillations and has a stabilizing effect on the aquatic ecosystem. Chakraborty et al. [5] propose in a

simple phytoplankton-nutrient model by considering the toxin release rate with a periodic function to reflect seasonal changes to highlight the dynamics of the seasonal plankton bloom mode. Their results concluded that with a varied release rate, the toxin can contribute to the explanation of algal blooms and a wide range of complex dynamic behaviors, such as simple cyclic blooms, irregular chaotic blooms, and jumping phenomena. This observation is made by varying the release rate of the toxin produced by the plankton. In the study of a toxic phytoplankton-zooplankton-phytoplankton model with a Monod-Haldane response function, Banerjee et al in [4, 5] exhibit the survival condition of zooplankton with phytoplankton in the presence of toxin. Therefore, it is very important to take into account toxins when studying zooplankton-phytoplankton interactions in the study of their dynamics. In 2024 recently, Shuo.Yao and all uses a modified Leslie-Gower predator-prey model to highlight the presence of periodic solutions via the Hopf bifurcation branching from the positive equilibrium with respect to two delays [14]. Despite these very interesting results in the literature, the real question of the release of the toxic in the aquatic environment with the permanent control of the parameter of the effectiveness of the toxin in the aquatic environment remains dark. This is why, using the Laplacian operator in polar coordinates, we formulate whith modified Leslie-Gower version type Holling II functional response a zooplankton-phytoplankton toxic model of spatial diffusion type in a circular domain that can control as a whole the instability caused by the toxin. To our knowledge, this type of model has never been addressed in the scientific literature.

In the treatment plan of this paper, we proceed to the formulation of a mathematical model of predator (zooplankton) and its prey (phytoplankton), based on a transformed version of Leslie-Gower. This model is governed by a system of two spatio-temporal equations on a circular domain (disc) with a functional response of the Benddington-Deangelis type. The mathematical analysis showed that the internal equilibrium state loses its stability producing the Turing and Hopf instability through the theoretical study of the bifurcation generating the formation of spatial patterns. These last results are illustrated by numerical simulations through which we observe that under the effect of the controlled toxin efficiency parameter, axial patterns appear and are very useful to understand the dynamics of the functioning of planktonic ecosystems [9, 10, 13].

2. Mathematical Model Formulation

2.1. Fundamental Model

Let us denote by H_z the average number of individuals in the zooplankton population representing the predator, H_p that of the phytoplankton representing the prey. Referring to [1, 8, 10], the dynamics of the general model is presented by the ordinary differential equation (ODE) in the form:

$$\begin{cases} \dfrac{dH_p}{dt} = J_1(H_p) - J_2(H_p, H_z)H_p, \\ \dfrac{dH_z}{dt} = J_3(H_p, H_z)H_z - J_4(H_p, H_z), \end{cases} \tag{1}$$

where

1. $J_1, J_2, J_3,$ and J_4 are positive functions and $\mathscr{C}^\infty$,
2. $J_1(H_p)$ is the growth function of the prey population in absence of predator,
3. $J_2(H_p, H_z)$ is the amount of prey consumed by a predator per time unit,
4. $J_3(H_p, H_z)$ the growth function of the predator population,
5. $J_4(H_p, H_z)$ predator population exploitation mortality and mortality due to toxin consumption. This mortality depends of the prey rate consumed by predator in the environment.

We continue the modelling by fixing the expressions of the functions intervening in the model (1).

$$J_1(H_p) = d_1 H_p - v_1 H_p^2,$$

$$J_2(H_p, H_z) = \frac{u_1 H_z}{H_p + e_1},$$

$$J_3(H_p, H_z) = d_2 H_z - \frac{d_3 H_z}{H_p + e_2},$$

$$J_4(H_p, H_z) = -u_2 H_z - \theta^p H_z$$

So we can illustrate the resulting dynamics of phytoplankton-zooplankton model with the diagram in figure 1 by considering the toxin effect in the two population and by setting $\widehat{u} = u_2 + \theta^p$.

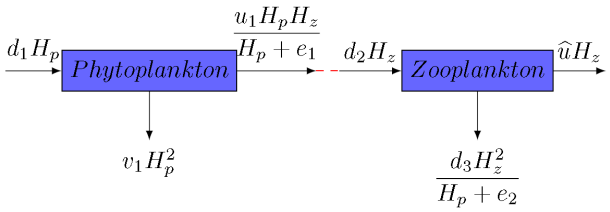

Figure 1. *Compartmental representation for phytoplankton-zooplankton interaction with toxin effect.*

Namely, according to the above assumptions and the interaction diagram in figure 1, the final ODE system used to model the evolution of prey and predators over time is given by:

$$\begin{cases} \dfrac{dH_p}{dt} = d_1 H_p - v_1 H_p^2 - \dfrac{u_1 H_z}{H_p + e_1} H_p, \\ \dfrac{dH_z}{dt} = d_2 H_z - \theta^p H_z - u_2 H_z - \dfrac{d_3 H_z^2}{H_p + e_2}, \\ H_p(0) = H_{p0} > 0, \quad H_z(0) = H_{z0} > 0, \end{cases} \tag{2}$$

1. d_1 is the phytoplankton growth rates,
2. v_1 is the mortality rate due to competition between the individuals of the phytoplankton population,
3. u_2 is the mortality rate due to the zooplankton population exploitation,
4. u_1 is the rate of predation for zooplankton,
5. d_3 is the zooplankton intraspecies competition mortality,
6. d_2 is the zooplankton growth rates,
7. θ^p is the mortality rate of the zooplankton due to the toxin liberation,
8. e_1 is the zooplankton half-saturation constant for a functional Holling type response,
9. e_2 is the fish half-saturation constant for a Holling type II functional response.

2.2. A Spatially Structured Model

In this section, we take into account the spatial structure in the previously implemented models. Thus, taking into account the possibility of species diffusion and climate, the system (1) is modeled as a spatial system with diffusion movements. By integrating the spatial diffusion terms into the system dynamics, our populations are now time and space dependent. Models containing diffusion are a simple and reasonable choice when modeling the dispersion of populations over a spatial domain, [1, 3, 10]. For the designation, $\delta_0(x,y)$, $\delta_1(x,y)$ be respectively the diffusion terms of H_p and H_z. In the same sense as the work established in [5, 10], the model of reaction-diffusion model associated with the model (1) can be represented for $(x,y) \in \Omega$ and $T \geq 0$ as follows:

$$\begin{cases} \partial_t H_p - \text{div}(\delta_0(x,y)\nabla H_p(T,x,y)) = J_1(H_p(T,x,y)) - J_2(H_p(T,x,y), H_z(T,x,y))H_z(T,x,y), \\ \partial_t H_z - \text{div}(\delta_1(x,y)\nabla H_z(T,x,y)) = J_3(H_z(T,x,y)) - J_4(H_p(T,x,y), H_z(T,x,y)); \ \ (x,y), \\ \nabla H_p(0,x,y).\eta = \nabla H_p(0,x,y).\eta = 0 \text{ on } \partial\Omega, \end{cases} \tag{3}$$

where

$$\Omega = \{(x,y) \in \mathbb{R}^2 / x^2 + y^2 < R^2\}$$

is the spatial domain in which species occur. We consider the zero-flux boundary condition:

$$\delta_i \nabla Q.\eta = 0, \ \ i = 0, 1, \ \ x \in \partial\Omega, \ \ T > 0$$

where η is the unit normal vector to $\partial\Omega$ on Ω and nonnegative initial and bounded conditions $Q(0,x,y) = Q_0(x,y) > 0, \ \ Q = H_p = W_p,$ or $Q = H_z = W_z, \ \ (x,y) \in \Omega$.So,

$$\begin{cases} \partial_t H_p = \left(d_1(x) - v_1(x)H_p - \dfrac{u_1(x)H_z}{H_p + e_1(x)} \right) H_p + \text{div}(\delta_0(x)\nabla H_p), \\ \partial_t H_z = \left(d_2(x) - \theta^p(x) - u_2(x) - \dfrac{d_3(x)H_z}{H_p + e_2(x)} \right) H_z + \text{div}(\delta_1(x)\nabla H_z). \end{cases} \tag{4}$$

Now, we suppose that all demographic parameters of system (4) are positive constants and the diffusion coefficients of system (4) are independent of the spatial variable. By considering $\delta_0(x,y) = \delta_0$, $\delta_1(x,y) = \delta_1$, model (4) previously obtained becomes:

$$\begin{cases} \dfrac{\partial H_p}{\partial t} = \left(d_1 - v_1 H_p - \dfrac{u_1 H_z}{H_p + e_1} \right) H_p + \delta_0 \Delta H_p, \ \ (x,y) \in \Omega, \ \ T \geq 0, \\ \dfrac{\partial H_z}{\partial t} = \left(d_2 - \theta^p - u_2 - \dfrac{d_3 H_z}{H_p + e_2} \right) H_z + \delta_1 \Delta H_z, \ \ (x,y) \in \Omega, \ \ T \geq 0, \\ \nabla H_p(0,x,y).\eta = \nabla H_z(0,x,y).\eta = 0 \text{ on } \partial\Omega. \end{cases} \tag{5}$$

Now, for $(x,y) \in \Omega$, we can write x and y in polar coordinates as follows $x = r\cos(\theta)$ and $y = r\sin(\theta)$ and the definition domain becomes

$$\mathcal{D} = \{(r,\theta) : 0 < r < R, 0 \leq \theta \leq 2\pi\},$$

where

$$r = \sqrt{x^2 + y^2} \ \text{ and } \ \tan(\theta) = \frac{y}{x}.$$

Without loss of generality we also denote $W_p(T,x,y) = W_p(T, r\cos(\theta), r\sin(\theta)) = W_p(t,r,\theta)$ and $W_z(T,x,y) = W_z(T, r\cos(\theta), r\sin(\theta)) = W_z(T,r,\theta)$ which are the densities of the phytoplankton and zooplankton respectively in polar coordinates. Therefore, the Laplacian in polar coordinates is given by:

$$\triangle_{r\theta} = \frac{\partial^2}{\partial r^2} + \frac{1}{r}\frac{\partial}{\partial r} + \frac{1}{r^2}\frac{\partial^2}{\partial \theta^2}.$$

Then, system (5) in polar coordinates at (T,r,θ) is:

$$\begin{cases} \dfrac{\partial W_p}{\partial T} = \left(d_1 - v_1 W_p - \dfrac{u_1 W_z}{W_p + e_1}\right) W_p(T,r,\theta) + \delta_0 \Delta_{r\theta} W_p(T,r,\theta), \\ \dfrac{\partial W_z}{\partial T} = \left(d_2 - \theta^p - u_2 - \dfrac{d_3 W_z}{W_p(T,r,\theta) + e_2}\right) W_z(T,r,\theta) + \delta_1 \Delta_{r\theta} W_z(T,r,\theta), \\ \forall\ (r,\theta) \in \mathcal{D} \text{ and } T > 0, \partial_r W_p(.,R,\theta) = \partial_r W_z(.,R,\theta) = 0, W_1(0,.,.) = W_p 0(.,.) \text{ and } W_z(0,.,.) = W_z 0(.,.). \end{cases} \tag{6}$$

3. Mathematical Results

3.1. Partial Results for the ODE System

3.1.1. Solution Boundary

we will give some essential results of the system (7) without the spatial diffusion on the circular domain. This result we will prepare for others in the framework of diffusion. Let us first note $\mathbb{R}^2_+ = \{(W_p, W_z) \in \mathbb{R}^2, W_p \geq 0, W_z \geq 0\}$. and

$$\text{int}(\mathbb{R}^2_+) = \{(W_p, W_z) \in \text{int}(\mathbb{R}^2), W_p(0) > 0, W_z(0) > 0\}.$$

Our population here will a priori be in these domains. We assume that our densities are always in these areas. We will then show that they are well defined for our populations.

Lemma 3.1. The quadrant int($\mathbb{R}^2$) is positively invariant of the system (7) Without spatial diffusion.

Proof. Let us first note that the limits of the nonnegative quadrant $\mathbb{R}^2_+$ are obviously invariant for the system (2) because $W_p(t) \geq 0$ and $W_z(t) \geq 0$ are positive for $t \geq 0$. So, $W_p(t) > 0$ and $W_z(t) > 0$ if $W_p(0) > 0$ and $W_z(0) > 0$. Therefore, the classical theorem of existence and uniqueness of differential equations ensures that the solutions are positive and that their axis cannot be crossed.

Lemma 3.2. For ω is an absolutely continuous function satisfying the differential inequality

$$\frac{d\omega(t)}{dt} + \lambda\omega(t) \leq \gamma, \ \ t \geq 0 \qquad (\lambda, \gamma) \in \mathbb{R}^2_+, \qquad \lambda \neq 0,$$

then

$$\forall t \geq \tau \geq 0, \quad \omega(t) \leq \frac{\gamma}{\lambda} - \left(\frac{\gamma}{\lambda} - \omega(\tau)\right) e^{-\lambda(t-\tau)}.$$

Theorem 3.1. Let us still consider the system (7) without spatial diffusion and let us denote by

$$\Sigma = \left[0, \frac{d_1}{v_1}\right] \times \left[0, \frac{1}{4d_3\nu_1}\left[d_3 d_1(d_1+4) + (d_1 + \nu_1 e_2)(d_2 - \theta^p + 1 - u_2)^2\right]\right],$$

and let us

$$M_1 = \frac{1}{4d_3\nu_1}\left[d_3 d_1(d_1+4) + (d_1 + \nu_1 e_2)(d_2 - \theta^p + 1 - u_2)^2\right].$$

Now we announce the following results:

1. The set Σ is positively invariant for the system (7) Without spatial diffusion.
2. Furthermore, all solutions of the system (2) initially taken in $\mathbb{R}^2_+$ are finally bounded with respect to $\mathbb{R}^2_+$ and end up entering the attractive set Σ.

Proof.

1. Let's define by $\Psi(t) = W_p(t) + w_z(t)$. By Lemma (3.1), if $(W_p(0), W_z(0)) \in \Sigma \subset \mathbb{R}^2_+$, then $(W_p(t), W_z(t))$ remain nonnegative. So, $(W_p(t), W_z(t)) \in \Sigma$. Now, we have to prove that for all $t \geq 0$, $0 \leq W_p(t) \leq \dfrac{d_1}{\nu_1}$ and $0 \leq W_p(t) + W_z(t) \leq M_1$.
   (a) First of all, since $(W_p(0), W_z(0)) > (0,0) \in Int(\mathbb{R}^2_+)$, all solution $(W_p(t), W_z(t))$ of system (2) initially starts Int($\mathbb{R}^2_+$), satisfies the differential inequality

$$\frac{W_p}{dt} \leq \left(d_1 - v_1 W_p(t) - \frac{u_1 W_z(t)}{W_p(t) + e_1}\right) W_p(t) \leq \frac{W_p}{dt} \leq W_p(t)\left(d_1 - v_1 W_p(t)\right).$$

   Considering the first equation of the system (2), thus $W_p(t)$ is similar to the solutions of $\dfrac{dv(t)}{dt} = v(t)\left(d_1 - v_1 v(t)\right), \quad v(0) = W_p(0) > 0$, with $v(t)$ expression is $v(t) = \dfrac{1}{\frac{\nu_1}{d_1} + ke^{-d_1 t}}$ where $k = \dfrac{1}{v(0)} - \dfrac{\nu_1}{d_1}$. Consequently, any solution $(W_p(t), W_z(t))$ nonnegative of system (2) satisfies $W_p(t) \leq \dfrac{d_1}{\nu_1}$, for $t \geq 0$.

(b) Now, the time derivative of $\Psi(t)$ is

$$\frac{d\Psi}{dt} = \frac{dW_p}{dt} + \frac{dW_z}{dt} = \left(d_1 - v_1 W_p - \frac{u_1 W_z}{W_p + e_1}\right) W_p + \left(d_2 - \theta^p - u_2 - \frac{d_3 W_z}{W_p + e_2}\right) W_z.$$

The parameters of the system being all positive and solutions initiating in $\mathbb{R}^2_+$, remain in the nonnegative quadrant, then

$$\frac{d\Psi}{dt} \leq (d_1 - v_1 W_p) W_p + \left(d_2 - \theta^p - u_2 - \frac{d_3 W_z}{W_p + e_2}\right) W_z$$

is verified, for all non-negative W_p and W_z. As the $(d_1 - v_1 W_p) W_p = \frac{d_1^2}{4\nu_1}$, then

$$\frac{d\Psi}{dt} \leq \frac{d_1^2}{4\nu_1} - \Psi + W_p + W_z + \left(d_2 - \theta^p - u_2 - \frac{d_3 W_z}{W_p + e_2}\right) W_z$$

and then

$$\frac{d\Psi}{dt} + \Psi \leq \frac{d_1^2}{4\nu_1} + \frac{d_1}{\nu_1} + \left(1 + d_2 - \theta^p - u_2 - \frac{d_3 \nu_1 W_z}{d_1 + \nu_1 e_2}\right) W_z,$$

since, in M_1, $0 \leq W_p \leq \frac{d_1}{\nu_1}$. By going to max, we get that

$$\left(1 + d_2 - \theta^p - u_2 - \frac{d_3 \nu_1 W_z}{d_1 + \nu_1 e_2}\right) W_z = \frac{1}{4 d_3 \nu_1}(d_1 + \nu_1 e_2)(d_2 - \theta^p + 1 - u_2)^2.$$

Finally, we get $\frac{d\Psi}{dt} + \Psi \leq M_1$. By fixing $\lambda = 1$ and $\gamma = M_1$, and using the lemma (3.2) we get,

$$\forall t \geq \tau \geq 0, \quad \omega(t) \leq M_1 - (M_1 - \omega(\tau))\, e^{-(t-\tau)}.$$

For $\tau = 0, \quad \omega(t) \leq M_1 - (M_1 - \omega(0))\, e^{-t}$. Hence, since $(W_p(0), W_z(0)) \in M_1, \Psi(t) = W_p(t) + w_z(t) \leq M_1,\ \forall t \geq 0$.

2. Now we will try to show that, for $(W_p(0), W_z(0)) \in \mathbb{R}^2_+$, $(W_p(t), W_z(t)) \longrightarrow M_1 \quad as \qquad t \longrightarrow +\infty$. Also, we will show that $\overline{lim}_{t \longrightarrow +\infty} W_p(t) \leq \frac{d_1}{\nu_1}$ and $\overline{lim}_{t \longrightarrow +\infty}(W_p(t) + W_z(t)) \leq M_1$.

   (a) First, $\overline{lim}_{t \longrightarrow +\infty} W_p(t) \leq \frac{d_1}{\nu_1}$ comes from 1, and lemma (3.2), since solutions of the initial value problem $\frac{dW_p(t)}{dt} = (d_1 - v_1 W_p(t))\, W_p(t), \quad W_p(0) \geq 0$, satisfies, $\overline{lim}_{t \longrightarrow +\infty} W_p(t) \leq \frac{d_1}{\nu_1}$.

   (b) Now, let $\epsilon > 0$, there exists $\tau_1 > 0$, such that $W_p(t) \leq 1 + \frac{\epsilon}{2}$ for $t \geq \tau_1 \geq 0$. By setting $\tau = \tau_1$, in the equation

$$\forall t \geq \tau \geq 0, \quad \omega(t) \leq M_1 - (M_1 - \omega(\tau))\, e^{-(t-\tau)},$$

we get $\forall t \geq \tau \geq 0, \quad \omega(t) \leq M_1 - (M_1 - \omega(\tau_1))\, e^{-(t-\tau_1)}$. Which gives

$$\omega(t) \leq M_1 - [M_1 e^{\tau_1} - (W_p(\tau_1) + W_z(\tau_1)) e^{\tau_1}]\, e^{-t} \leq M_1 - [M_1 - (W_p(\tau_1) + W_z(\tau_1)) e^{\tau_1}]\, e^{-t}.$$

Then

$$\omega(t) = (W_p(t) + W_z(t)) \leq (M_1 + \frac{\epsilon}{2}) - \left[(M_1 + \frac{\epsilon}{2}) - (W_p(\tau_1) + W_z(\tau_1)) e^{\tau_1}\right] e^{-t}, \qquad \forall t \geq \tau_1 \geq 0.$$

For $\tau_2 \geq \tau_1$ such that,

$$\left[(M_1 + \frac{\epsilon}{2}) - (W_p(\tau_1) + W_z(\tau_1)) e^{\tau_1}\right] e^{-t} \leq \frac{\epsilon}{2} \qquad \forall t \geq \tau_2.$$

We conclude that

$$W_p(t) + W_z(t) \leq M_1 + \frac{\epsilon}{2} \qquad \forall t \geq \tau_2.$$

As a result

$$\overline{lim}_{t\longrightarrow+\infty} W_p(t) + W_z(t) \leq M_1.$$

3.2. Polar Coordinates System Study

Now, consider the system(7) in polar coordinates in its circular domain:

$$\begin{cases} \dfrac{\partial W_p(t,r,\theta)}{\partial t} = \left(d_1 - v_1 W_p(t,r,\theta) - \dfrac{u_1 W_z(t,r,\theta)}{W_p(t,r,\theta)+e_1}\right) W_p + \delta_0 \Delta_{r\theta} W_p(t,r,\theta); \ \ \forall\, (r,\theta) \in \mathcal{D} \text{ and } t>0, \\ \dfrac{\partial W_z(t,r,\theta)}{\partial t} = \left(d_2 - \theta^p - u_2 - \dfrac{d_3 W_z(t,r,\theta)}{W_p(t,r,\theta)+e_2}\right) W_z + \delta_1 \Delta_{r\theta} W_z(t,r,\theta); \\ \forall\, (r,\theta) \in \mathcal{D} \text{ and } t>0, \ \ \partial_r W_p(.,R,\theta) = \partial_r W_z(.,R,\theta) = 0. \end{cases} \tag{7}$$

By converting this writing to mathematical uses, we have

$$\begin{cases} \dfrac{\partial X_1}{\partial t} = \left(d_1 - v_1 X_1 - \dfrac{u_1 X_2}{X_1+e_1}\right) X_1 + \delta_0 \Delta_{r\theta} X_1 = f_1(X_1,X_2) + \delta_0 \Delta_{r\theta} W_p(t,r,\theta), \\ \dfrac{\partial X_2}{\partial t} = \left(d_2 - \theta^p - u_2 - \dfrac{d_3 X_2}{X_1+e_2}\right) X_2 + \delta_1 \Delta_{r\theta} X_2 = g_1(X_1,X_2) + \delta_1 \Delta_{r\theta} W_p(t,r,\theta), \end{cases} \tag{8}$$

and without the polar coordinates, we have

$$\begin{cases} \dfrac{dY_1}{dt} = \left(d_1 - v_1 Y_1 - \dfrac{u_1 B_2}{Y_1+e_1}\right) Y_1 = f_1(Y_1,Y_2), \\ \dfrac{dY_2}{dt} = \left(d_2 - \theta^p - u_2 - \dfrac{d_3 Y_2}{Y_1+e_2}\right) Y_2 = g_1(Y_1,Y_2). \end{cases} \tag{9}$$

3.3. Existence and Boundedness of Solution

Let us first give the bounded domain of our polar system (7).

Theorem 3.2. (i) The set Γ is a positively invariant region for the system (7), where

$$\Gamma = \left[0, \frac{d_1}{v_1}\right] \times \left[0, \frac{l_1}{d_3 v_1}(d_1 + v_1 e_2)\right].$$

(ii) All solutions of system (7) initiating in Γ are bounded and enter the attraction region Γ.

(iii) The domain $\mathbb{R}^+ \times \mathbb{R}^+$ is positively invariant for the system (7). Furthermore, any solution of the system (7) whose initial condition is in $\mathbb{R}^+ \times \mathbb{R}^+$, converges to the set defined by

$$\Gamma = \left[0, \frac{d_1}{v_1}\right] \times \left[0, \frac{l_1}{d_3 v_1}(d_1 + v_1 e_2)\right] \subset \left[0, \frac{d_1}{v_1}\right] \times \left[0, \frac{1}{4 d_3 \nu_1}\left[d_3 d_1 (d_1+4) + (d_1 + \nu_1 e_2)(d_2 - \theta^p + 1 - u_2)^2\right]\right].$$

Proof.

(i) Let us first note that $(0,0)$ is a sub-solution of the problem (7). We then have, $X_1(t,r,\theta) > 0$ and $X_2(t,r,\theta) > 0$ as soon as $X_1(0)(r,\theta) > 0$ and $X_2(0)(r,\theta) > 0$. Then int$(\mathbb{R}^2_+)$ is invariant by the system (7) (see lemma 3.1). Now, for $(X_1(0)(r,\theta), X_2(0)(r,\theta)) \in \Gamma$, since int$(\mathbb{R}^2_+)$, then the solution $(X_1(t)(r,\theta), X_2(t)(r,\theta))$ using the initial condition $(X_1(0), X_2(0))$ is positive and for any $t \geq 0$, we have $X_1(t) \leq \dfrac{d_1}{v_1}$ and $X_2(t) \leq \dfrac{l_1}{d_3 v_1}(d_1 + v_1 e_2)$.

(ii) Given $(X_1(t)(r,\theta), X_2(t)(r,\theta))$ a positive solution of (7), we have

$$\begin{cases} \dfrac{\partial X_1(t,r,\theta)}{\partial t} \leq (d_1 - v_1 X_p(t,r,\theta)) X_1(t,r,\theta), \\ \dfrac{\partial X_1(.,r,\theta)}{\partial r} = 0, \\ X_1(0,r,\theta) = X_1 0(r,\theta) \leq \max\limits_{(r,\theta)\in\overline{D}} X_1 0(r,\theta) \end{cases} \tag{10}$$

Applying the comparison principle as in the case of the lemma (3.2), we deduce that

$$\lim_{t\longrightarrow+\infty} \sup\ W_1(t)(r,\theta) \leq \frac{d_1}{v_1}. \tag{11}$$

So, for all $\epsilon > 0$, there exists $T > 0$ such that

$$X_1(t)(r,\theta) \leq \frac{d_1}{v_1} + \epsilon \ \text{ for } \ t \geq T. \tag{12}$$

According to system (7), we have

$$\begin{cases} \dfrac{\partial X_2(t,r,\theta)}{\partial t} \leq \left(l_1 - \dfrac{d_3 X_1(t,r,\theta)}{X_1(t,r,\theta)+e_2}\right) X_2(t,r,\theta), \\ \\ X_1(0) = X_1 0 \geq 0. \end{cases} \tag{13}$$

From the second equation of system (7), we have

$$\begin{cases} \dfrac{\partial X_2(t,r,\theta)}{\partial t} \leq \left(l_1 - \dfrac{d_3 X_2(t,r,\theta)}{X_2(t,r,\theta)+e_2}\right) X_2, \\ \dfrac{\partial X_1(.,r,\theta)}{\partial r} = 0, \\ X_1(0,r,\theta) = X_1 0(r,\theta) \leq \max\limits_{(r,\theta)\in\overline{D}} X_1 0(r,\theta). \end{cases} \tag{14}$$

According to lemma (3.2) and the expression (7), we have

$$\frac{\partial X_2(r,\theta)}{\partial t} \leq \left(l_1 - \frac{d_3 X_2(r,\theta)}{\dfrac{d_1}{v_1} + \epsilon + e_2}\right) X_2(r,\theta), \text{ for } t \geq T.$$

By tending ϵ towards 0, we have clearly

$$\lim_{t\longrightarrow+\infty} \sup X_2(t)(r,\theta) \leq \frac{d_1}{v_1 d_3}(d_1 + v_1 e_2), \tag{15}$$

that gives the result.

(iii) For initial condition $(X_1(0)(r,\theta), X_2(0)(r,\theta))$ of the system (7), we have

$$0 \leq X_1 \leq Y_1, \ \ Y_1(0) = max_{\overline{\Omega}}\ X_1(0)(r,\theta)$$

$$0 \leq X_2 \leq Y_2, \ \ Y_2(0) = max_{\overline{\Omega}}\ X_2(0)(r,\theta).$$

$$\frac{\partial X_2}{\partial t} = \left(l_1 - \frac{d_3 X_2}{X_1 + e_2}\right) X_2 + \delta_1 \Delta_{r\theta} X_2,$$

and we obtain the following inequality: $\dfrac{\partial X_2}{\partial t} \leq \frac{dY_2}{dt}$ where Y_2 is solution of the second equation of the system (9) with initial condition $Y_2(0) = max_{\overline{\Omega}}\ X_2(0)(r,\theta)$.

$$\frac{\partial X_2}{\partial t} \leq \frac{dY_2}{dt} + \frac{dY_1}{dt}$$

Consider $\omega = Y_2 + Y_1$ in the Lemma (3.2), we deduce that

$$\frac{\partial X_2}{\partial t} \leq \frac{d\sigma}{dt} \leq \frac{1}{4d_3\nu_1}\left[d_3 d_1(d_1+4) + (d_1 + \nu_1 e_2)(d_2 - \theta^p + 1 - u_2)^2\right].$$

Using the Gronwal Lemma [10], we deduce that $X_2 \leq \dfrac{1}{4d_3\nu_1}\left[d_3 d_1(d_1+4) + (d_1 + \nu_1 e_2)(d_2 - \theta^p + 1 - u_2)^2\right] - \omega.$

Thus, the solutions X_1 and X_2 are bounded. On the other hand, according to lemma (3.2), we have

$$\overline{\lim}_{t\longrightarrow+\infty} Y_1(t) \leq d_1/v_1$$

and

$$\overline{\lim}_{t\longrightarrow+\infty}(Y_1(t)+Y_2(t)) \leq \frac{1}{4d_3\nu_1}\left[d_3d_1(d_1+4)+(d_1+\nu_1e_2)(d_2-\theta^p+1-u_2)^2\right].$$

3.3.1. Model Equilibrium Points

Let us adopt the following change of variables:

$$r_1 = d_2-\theta^p-u_2,\ W_p(t)=\frac{\nu_1}{d_1}H_p(T), W_z(t)=\frac{\nu_1 d_3}{d_1 r}H_z(T),\ t=d_1T,\ a=\frac{r_1u_1}{d_1\alpha_2},$$

$$b=\frac{r_1}{d_1},\ \gamma_1=\frac{\nu_1e_1}{d_1},\ \gamma_2=\frac{\nu_0e_2}{d_1},\ r'=r\left(\frac{d_1}{\delta_0}\right)^{\frac{1}{2}},\ \theta'=\theta\left(\frac{d_1}{\delta_0}\right)^{\frac{1}{2}},\ \delta_{zp}=\frac{\delta_1}{\delta_0}.$$

The following results give the stationaries states (and their stability condition) of the system (7). The following result gives the stationaries states and their stability condition of the system (7).

Proposition 3.1.
1. $E_0=(0,0)$ is the trivial state. This equilibrium is unstable.
2. $E_1=(1,0)$ is an equilibrium point. This equilibrium is unstable.
3. $E_2=(0,\gamma_2)$ is an equilibrium point.

Theorem 3.3.
1. The equilibrium point $E_0=(0,0)$ is an unstable node.
2. The equilibrium point$E_1=(1,0)$ is a saddle point.
3. $E_2=(0,\gamma_2)$ is unstable state if $\gamma_1>a\gamma_2$ and stable if $\gamma_1<a\gamma_2$. Moreover, a local bifurcation appears as soon as we have equality $\gamma_1=a\gamma_2$.

We will make the following hypothesis: (H_1) : $a \geq \dfrac{1}{2(1+\gamma_2)}$ and $0<\gamma_1<\overline{\gamma}_1$ with $\overline{\gamma}_1=-(a+1)+\sqrt{\xi}$, $\xi=(a+1)^2+2a(1+2a)-1$.

Theorem 3.4. The interior equilibrium point $E_3=(W_P^*(t,r,\theta),W_Z^*(t,r,\theta))$ of the system (7) is stable if the hypothesis (H_1) is satisfied.

Proof. Concerning the proof of the local stability of E_i, we solve by considering the eigenvalue problem of the corresponding linearized operator. In fact, we consider $(W_p(t,r,\theta),W_z(t,r,\theta))$ the solution of the system (7), then, we have $(W_p(t,r,\theta),W_z(t,r,\theta))=E_i+U(t,r,\theta)=E_i+(U_1(t,r,\theta),U_2(t,r,\theta))$. Let ϕ_j be the j^{ieme} eigenfunction defined on Ω, of the following system whose associated operator is $-\Delta$.

$$\begin{cases} -\Delta\phi_j(t,r,\theta)=\lambda_j\phi_j(r,\theta) \text{ on } \mathcal{D},\\ \dfrac{\partial\phi_j}{\partial\nu}\mid_{\partial\mathcal{D}} =0, \text{ on } \partial\mathcal{D}, \end{cases} \tag{16}$$

where the λ_j are the eigenvalue satisfying $0=\lambda_0<\lambda_1<\lambda_2<...$ From the system (7), the linearized system of the system (7) at (W_p^*,W_z^*) is

$$\frac{\partial U}{\partial t}=D\Delta U+\Sigma U, \tag{17}$$

with $D=\text{diag}(\gamma_1,\gamma_2)$, and

$$\Sigma=\begin{pmatrix} A_0 & B\\ Q & R\end{pmatrix}=\begin{pmatrix} 1-2W_p^*-\dfrac{\gamma_1(1-W_p^*)}{W_p^*+\gamma_1} & -\dfrac{aW_p^*}{W_p^*+\gamma_1}\\ b & -b\end{pmatrix}. \tag{18}$$

The developed expression of the U solution of (17) is the following

$$U=\sum_{j=0}^{\infty} z_j(t)\phi_j(r,\theta), \tag{19}$$

where each $z_j(t)\in\mathbb{R}^2$. From the expressions (19) and (17), we have $\dfrac{\delta pz_j}{dt}=C_jz_j$, where $C_j=L\Sigma-\lambda_jD$. Thus, the homogeneous equilibrium (W_p^*,W_z^*) is stable if and only if each $z_j(t)$ decreases to zero. This is equivalent to saying that all the eigenvalues of each C_j are negative real parts. The eigenvalues $\eta_{1,2}$ of C_j are determined by solving the following equation $\eta^2-\rho\left(A_0+R-\lambda_j(\gamma_1+\gamma_2)\right)+\lambda_j^2\gamma_1\gamma_2-\lambda_j(\gamma_1R+\gamma_2A_0)+A_0R-BQ=0$. Consequently, the real part of each eigenvalue of C_j is negative if we have

$$A_0+R-\lambda_j(\gamma_1+\gamma_2)<0, \text{ and } \lambda_j^2\gamma_1\gamma_2-\lambda_j(\gamma_1R+\gamma_2A_0)+A_0R-BQ>0. \tag{20}$$

Note that $R = -b < 0, \lambda_j \geq 0$ and $B < 0$.
Therefore, the condition (20) is satisfied if $A_0 \leq 0$, and $Q > 0$. If $A_0 \leq 0$, it is sufficient that $2U_1^* - 1 - \gamma_1 \geq 0$ and $1 - a - \gamma_1 + \sqrt{\Delta} - 1 + \gamma_1 \geq 0$. This implies $\Delta \geq a$ and consequently $(a - \gamma_1 - 1)^2 - 4(a\gamma_2 - \gamma_1) - \gamma^2 \geq a$ $\gamma_1^2 + (2\gamma_1 + 2)\gamma_1 - 2\gamma(1 + 2\gamma_2) + 1 \geq 0$. Now, these two inequalities are verified according to (H_3), so $A_0 \leq 0$. On the other hand, $Q > 0$ and consequently the interior equilibrium (W_p^*, W_z^*) is stable.

Theorem 3.5. If the conditions $u_1 < \frac{d_1}{\nu_1}$ and $e_2 - M_2 - u_1 + \frac{d_1}{\nu_1} > 0$ are satisfied, then the system (7) admits at least one positive solution $(X_1(r,\theta), X_2(r,\theta))$, where M_2 is a sub-solution of the second equation of the system (7).

Proof. We write the system (7) as follows:

$$\begin{cases} \dfrac{\partial X_1}{\partial t} = \left(d_1 - v_1 X_1 - \dfrac{u_1 X_2}{X_1 + e_1}\right) X_1 + \delta_0 \Delta_{r\theta} X_1 = f_1(X_1, X_2) + \delta_0 \Delta_{r\theta} X_1, \\ \dfrac{\partial X_2}{\partial t} = \left(d_2 - \theta^p - u_2 - \dfrac{d_3 X_2}{X_1 + e_2}\right) X_2 + \delta_1 \Delta_{r\theta} X_2 = g_1(X_1, X_2) + \delta_1 \Delta_{r\theta} X_2, \end{cases} \tag{21}$$

and

$$\begin{cases} -\delta_0 \Delta_{r\theta} \underline{X}_1 = \left(d_1 - v_1 X_1 - \dfrac{u_1 X_2}{X_1 + + e_1}\right) X_1 = f_1, \\ -\delta_1 \Delta_{r\theta} \underline{X}_2 = \left(d_2 - \theta^p - u_2 - \dfrac{d_3 X_2}{X_1 + e_2}\right) X_2 = g_1, \\ \forall\, (r,\theta) \in \mathcal{D} \text{ and } t > 0, \ \ \partial_r X_1 = \partial_r X_2 = 0. \end{cases} \tag{22}$$

If $X_1(r,\theta) \geq 0, X_2(r,\theta) \geq 0, \quad t \geq 0$, we obtain

$$\frac{\partial f_1}{\partial X_2} = -\frac{u_1 X_1}{X_1 + e_1} \leq 0, \frac{\partial g_1}{\partial X_1} = \frac{d_3 X_2^2}{(X_1 + e_2)^2} \geq 0.$$

This means that the function f_1 is quasi-monotone decreasing and the function g_1 is quasi-monotone increasing. The system (7) is then called a quasi-monotonic mixed system. We will now construct a pair of over-solution and sub-solution of the system (7) that we denote respectively by

$$\varphi_1 = (\overline{X}_1(r,\theta), \overline{X}_2(r,\theta)) \text{ and } \varphi_2 = (\underline{X}_1(r,\theta), \underline{X}_2(r,\theta)).$$

Let us remember that, $\varphi_1(r,\theta)$ is an over-solution and $\varphi_2(r,\theta)$ is a sub-solution of the system (7) if we have

$$\frac{\overline{X}_1}{\partial r} \geq 0 \geq \frac{\underline{X}_1}{\partial r} \text{ on } \partial\, \mathcal{D}, \frac{\overline{X}_2}{\partial r} \geq 0 \geq \frac{\underline{X}_2}{\partial r} \text{ on } \partial\, \mathcal{D},$$

and

$$-\delta_0 \Delta_{r\theta} \overline{X}_1 - d_1 \overline{X}_1 \left(1 - \frac{\nu_1}{d_1} \overline{X}_1 - \frac{u_1 \overline{X}_2}{d_1 \overline{X}_1 + d_1 e_1}\right) \geq 0 \geq -\delta_0 \Delta_{r\theta} \underline{X}_1 - d_1 \underline{X}_1 \left(1 - \frac{\nu_1}{d_1} \underline{X}_1 - \frac{u_1 \underline{X}_2}{d_1 \underline{X}_1 + d_1 e_1}\right) \tag{23}$$

$$-\delta_0 \Delta_{r\theta} \overline{X}_2 - l_1 \overline{X}_2 \left(1 - \frac{d_3 \overline{X}_2}{l_1 \overline{X}_1 + l_1 d_2}\right) \geq 0 \geq -\delta_1 \Delta_{r\theta} \underline{X}_1 - l_1 \underline{X}_2 \left(1 - \frac{d_3 \underline{X}_2}{l_1 \underline{X}_1 + l_1 d_2}\right). \tag{24}$$

Let $\overline{X}_1(r,\theta) = \frac{d_1}{\nu_1}$, then for every $\overline{X}_2(r,\theta) \geq 0$, the first inequality of (7) is satisfied. By fixing M_2 such that

$$M_2 \geq \frac{1}{4 d_3 \nu_1} \left[d_3 d_1 (d_1 + 4) + (d_1 + \nu_1 e_2)(d_2 - \theta^p + 1 - u_2)^2\right]$$

and by considering $\overline{X}_2(x) = M_2$, the inequality of (24) is satisfied. If we consider that $\overline{X}_2(x) = M_2$, the second inequality of (23) becomes

$$-\delta_0 \Delta_{r\theta} \underline{X}_1 - d_1 \underline{X}_1 \left(1 - \frac{\nu_1}{d_1} \underline{X}_1 - \frac{u_1 \underline{X}_2}{d_1 \underline{X}_1 + d_1 e_1}\right) \leq 0.$$

Let $\underline{X}_1(r,\theta)$ the strictly positive solution of the following system:

$$\begin{cases} \delta_0 \Delta_{r\theta} \underline{X}_1 - d_1 \underline{X}_1 \left(1 - \dfrac{\nu_1}{d_1}\underline{X}_1 - \dfrac{u_1 \underline{X}_2}{d_1 \underline{X}_1 + d_1 e_1}\right) = 0, \\ \partial_r X_1(., R, \theta) = 0. \end{cases} \tag{25}$$

We will show that if the conditions $u_1 < \dfrac{d_1}{\nu_1}$ and $e_2 - M_2 - u_1 + \dfrac{d_1}{\nu_1} > 0$ are satisfied, then the system (25) will admit a positive solution. If $u_1 < \dfrac{d_1}{\nu_1}$ and $e_2 - M_2 - u_1 + \dfrac{d_1}{\nu_1} > 0$ then one can easily verify that $(\dfrac{d_1}{\nu_1}; \dfrac{d_1}{\nu_1} - u_1)$ is a pair of over-solution and sub-solution of the equation (25). This equation admits a positive solution $\underline{X}_1(r, \theta)$ which checks $\left(\dfrac{d_1}{\nu_1} - u_1\right) \leq \underline{U}_1(r, \theta) \leq \dfrac{d_1}{\nu_1}$. Obviously, we have

$$\overline{X}_1(r, \theta) \geq \underline{X}_1(r, \theta).$$

We give ourselves arbitrarily $\overline{X}_1(r, \theta)$, $\underline{X}_1(r, \theta)$ and $\underline{X}_2(r, \theta)$. If $e_2 - M_2 - u_1 + \dfrac{d_1}{\nu_1} > 0$ then we can choose $\underline{X}_2(r, \theta)$ constant positive and small enough so that the following inequality is satisfied:

$$-\delta_0 \Delta_{r\theta} \underline{X}_1 - d_1 \underline{X}_1 \left(1 - \frac{\nu_1}{d_1}\underline{X}_1 - \frac{u_1 \underline{X}_2}{d_1 \underline{X}_1 + d_1 e_1}\right) \leq 0$$

Note that this inequality is satisfied as soon as $0 < \underline{X}_2 < 1 - a - d_2$. Thus we build a pair of over-solution and sub-solution $(\overline{X}_1(r, \theta), \overline{X}_2(r, \theta))$ and $(\underline{X}_1(r, \theta), \underline{X}_2(r, \theta))$ of the system (7).

Thus, the system (7) admits at least one solution $(X_1(r, \theta), X_2(r, \theta))$ which satisfies

$$\underline{X}_1(r, \theta) \leq X_1(r, \theta) \leq \overline{X}_1(r, \theta)$$

$$\underline{X}_2(r, \theta) \leq X_2(r, \theta) \leq \overline{X}_2(r, \theta) \qquad \square$$

$\gamma_1 > a\gamma_2$ and stable if $\gamma_1 < a\gamma_2$. Moreover, a local bifurcation appears as soon as we have equality $\gamma_1 = a\gamma_2$.

Theorem 3.6. If the hypotheses $\gamma_1 > a\gamma_2$ and $\gamma_2 \geq \gamma_1 \geq 1 > a > 0$, then the equilibrium $E^* = (W_p^*, W_z^*)$ of the system (7) is globally asymptotically stable.

Proof. Let us consider now, the functions l and L defined by

$$l(W_p, W_z) = \int_{W_p^*}^{W_p} \frac{(\eta - W_p^*)(\eta + \gamma_1)}{a\eta(\eta + \gamma_2)} d\eta + \frac{W_p^* + \gamma_2}{bW_z^*} \int_{W_z^*}^{W_z} \frac{\eta - W_z^*}{\eta} d\eta.$$

Let us now define the functions f and g as the reaction terms of system (7) such that

$$\begin{cases} \dfrac{\partial W_p(t, r, \theta)}{\partial t} = f(t, r, \theta) + \delta_0 \Delta_{r\theta} W_p(t, r, \theta), \dfrac{\partial W_z(t, r, \theta)}{\partial t} = g(t, r, \theta) + \delta_1 \Delta_{r\theta} W_z(t, r, \theta), \\ \partial_r W_p(., R, \theta) = \partial_r W_z(., R, \theta) = 0,\ W_p(0, ., .) = W_p 0(., .), W_z(0, ., .) = W_z 0(., .). \end{cases} \tag{26}$$

Using the relation $\displaystyle\int_{\mathcal{D}} f(\rho) d\rho = \int_0^R \int_0^{2\pi} f(r, \theta) d\theta dr$, we have

$$L(W_p, W_z) = \int_{\mathcal{D}} l(W_p(t, \rho), W_z(t, \rho)) d\rho$$

$$= \int_{\mathcal{D}} \left(\int_{W_p^*}^{W_p(t,\rho)} \frac{(\eta - W_p^*)(\eta + \gamma_1)}{a\eta(\eta + \gamma_2)} d\eta \right) d\rho + \int_{\mathcal{D}} \left(\frac{W_p^* + \gamma_2}{bW_z^*} \int_{W_z^*}^{W_z(t,\rho)} \frac{\eta - W_p^*}{\eta} d\eta \right) d\rho.$$

Our goal is to show that L is a Lyapunov function. Indeed, for any (W_p, W_b) in the positive quadrant $\mathbb{R}^2_{*+}$, $L(W_p, W_z)$ is positive and $L(W_p^*, W_z^*) = 0$. In the other hand, we have:

$$\begin{aligned} \frac{dL}{dt} &= \int_{\mathcal{D}} \left(\frac{\partial l}{\partial W_p} \frac{\partial W_p}{\partial t} + \frac{\partial l}{\partial W_z} \frac{\partial W_z}{\partial t} \right) d\rho, \\ &= \int_{\mathcal{D}} \left(\frac{\partial l}{\partial W_p} (\delta_0 \Delta W_p + f(W_p, W_z)) \right) d\rho + \int_{\mathcal{D}} \left(\frac{\partial l}{\partial W_z} (\delta_1 \Delta W_z + g(W_p, W_z)) \right) d\rho \\ &= \int_{\mathcal{D}} \left(\delta_0 \frac{\partial l}{\partial W_p} \Delta W_p + \delta_1 \frac{\partial l}{\partial W_z} \Delta W_z \right) d\rho + \int_{\mathcal{D}} \left(\frac{\partial l}{\partial W_p} f(W_p, W_z) + \frac{\partial l}{\partial W_z} g(W_p, W_z) \right) d\rho \\ &= \int_{\mathcal{D}} \left(\delta_0 \frac{\partial l}{\partial W_p} \Delta W_p + \delta_1 \frac{\partial l}{\partial W_z} \Delta W_z \right) d\rho + \int_{\mathcal{D}} \frac{\partial l}{\partial t} d\rho \end{aligned}$$

By using the formula of Green,

$$\int_{\mathcal{D}} \delta_0 \frac{\partial l}{\partial W_p} \Delta W_p d\rho \quad = \quad \delta_0 \left(\int_{\partial \mathcal{D}} \frac{\partial l}{\partial W_p} \frac{\partial W_p}{\partial \eta} - \int_{\mathcal{D}} \nabla \frac{\partial l}{\partial W_p} \nabla W_p d\rho \right) = -\delta_0 \int_{\mathcal{D}} \nabla \frac{\partial l}{\partial W_p} \nabla W_p d\rho$$

and

$$\int_{\mathcal{D}} \delta_1 \frac{\partial l}{\partial W_z} \Delta W_z d\rho = \delta_1 \left(\int_{\partial \mathcal{D}} \frac{\partial l}{\partial W_z} \frac{\partial W_z}{\partial \eta} - \int_{\mathcal{D}} \nabla \frac{\partial l}{\partial W_z} \nabla W_z d\rho \right) = -\delta_1 \int_{\mathcal{D}} \nabla \frac{\partial l}{\partial W_z} \nabla W_z d\rho$$

where

$$\nabla_{r\theta} W_p = \left(\frac{\partial W_p}{\partial r}, \frac{1}{r} \frac{\partial W_p}{\partial \theta} \right).$$

Let us denote by

$$T_1(W_p) = \int_{W_p^*}^{W_p} \frac{(\eta - W_p^*)(\eta + \gamma_1)}{u_1 \eta (\eta + \gamma_2)} d\eta \text{ and } T_2(W_2^b) = \frac{W_p^* + \gamma_2}{b W_z^*} \int_{W_z^*}^{W_z} \frac{\eta - W_p^*}{\eta} d\eta.$$

After a simple calculation followed by a reduction,

$$T_1^{"}(W_p) = \frac{1}{a}((W_p^* + \gamma_2 - \gamma_1) W_p^2 + 2(\gamma_2 W_p^* W_z^* + \frac{1}{2}\gamma_1 \gamma_2 W_p^*)) T_2^{"}(W_z) = \frac{W_p^* + \gamma_2}{b W_z^*} \cdot \frac{W_z^*}{W_z^2} \geq 0.$$

Using the hypothesis $\gamma_1 > a\gamma_2$ and $\gamma_2 \geq \gamma_1 \geq 1 > a > 0$, we get $T_1^{"} \geq 0$. Therefore, the matrix

$$\begin{pmatrix} \frac{\partial^2 l}{\partial W_p^2} & \frac{\partial^2 l}{\partial W_p \partial W_z} \\ \frac{\partial^2 l}{\partial W_p \partial W_z} & \frac{\partial^2 l}{\partial W_z^2} \end{pmatrix},$$

is positive definite and we have

$$\int_{\mathcal{D}} \left(\delta_0 \frac{\partial l}{\partial W_p} \Delta W_p + \delta_0 \frac{\partial l}{\partial W_z} \Delta W_z \right) d\rho \leq 0.$$

According to $\frac{\partial l}{\partial t} \leq 0$ due to the hypotheses $\gamma_1 > a\gamma_2$ and $\gamma_2 \geq \gamma_1 \geq 1 > a > 0$, we have $\frac{dL}{dt}(W_p, W_z) \leq 0$. Therefore, according to the theorem of LaSalle's [4, 10], the equilibrium point (W_p^*, W_z^*) is globally asymptotically stable.

3.4. Bifurcation Analysis

For the formation of spatio-temporal patterns, there are two types of classical bifurcations. The bifurcation of Hopf breaks the temporal symmetry of the system and leads to uniform oscillations in space and periodicals. Turing's bifurcation breaks spatial symmetry and leads to pattern formation stationary in time and oscillatory in space [6, 10, 14]. Let

$$V = \begin{pmatrix} W_p - W_p^* \\ W_z - W_z^* \end{pmatrix} \varphi(r, \theta) e^{\lambda t + i\zeta r},$$

where ζ is the wave number and $\varphi(r, \theta)$ is a proper vector of the Laplace operator on the circular domain $\mathcal{D}$ i.e:

$$\begin{cases} \Delta_{r\theta} \varphi = -\zeta^2 \varphi, \\ \varphi_r(R, \theta) = 0. \end{cases} \tag{27}$$

Then, by linearizing around $E^*(W_p^*, W_z^*)$, we have the following equation:

$$\frac{dV}{dt} = J(E^*)V + D\Delta V \tag{28}$$

where

$$J(E^*) = \begin{pmatrix} f_{W_p^*} & f_{W_z^*} \\ g_{W_p^*} & f_{W_z^*} \end{pmatrix} = \begin{pmatrix} 1 - 2W_p^* - \frac{\gamma_1(1 - W_p^*)}{W_p^* + \gamma_1} & -\frac{aW_p^*}{W_p^* + \gamma_1} \\ b & -b \end{pmatrix},$$

$$D = \begin{pmatrix} \delta_0 & 0 \\ 0 & \delta_1 \end{pmatrix}.$$

By linearization around $E^*(W_p^*, W_z^*)$, we find the following characteristic equation

$$\Phi(\zeta^2) = \lambda^2 + M_1(\zeta^2)\lambda + M_2(\zeta^2), \tag{29}$$

where

$$M_1(\zeta^2) = \zeta^2(\delta_0 + \delta_1) - \text{tr}(J(E^*)), \tag{30}$$

$$M_2(\zeta^2) = \delta_0\delta_1\zeta^4 - (\delta_0 f_{W_p^*} + \delta_0 g_{W_z^*})\zeta^2 + det(J(E^*)). \tag{31}$$

$$\lambda_{\pm}(\zeta) = \frac{-M_1(\zeta^2) \pm \sqrt{(M_1(\zeta^2))^2 - 4M_2(\zeta^2)}}{2}. \tag{32}$$

(H_2): $b + \gamma_1 > 1$, or $0 < W_p^* < \theta_1$, or $\theta_2 < W_p^*$ and $\delta_1 < (\delta_1)_c$, where

$$(\delta_1)_c = \frac{-(2f_{W_z^*}g_{W_p^*} - f_{W_z^*}g_{W_p^*})}{f_{W_z^*}^2} + \frac{2\sqrt{(f_{W_z^*}g_{W_p^*} - f_{W_p^*}g_{W_z^*})^2 - f_{W_p^*}^{*2}g_{W_z}^{*2} + f_{W_z^*}g_{W_p^*}f_{W_p^*}g_{W_z^*}}}{f_{W_z^*}^2}.$$

Theorem 3.7. If hypothesis (H_2) is satisfied and $\delta_1 < (\delta_1)_c$, then $E^* = (W_p^*, W_z^*)$ is asymptotically stable for the system (2) If $\delta_1 > (\delta_1)_c$, then $E^* = (W_p^*, W_z^*)$ is unstable for the system (7).

Remark 3.1. For $\zeta^2 = 0$, the characteristic equation (29) is written:$\Phi(0) = \lambda^2 - \mathrm{tr}(J(E^*))\lambda + \det(J(E^*))$ that coincides with the characteristic equation of equation (28) without diffusion.

Proposition 3.2. The hypothesis (H_1) and (H_2) are the necessaries conditions to give Turing and Hopf patterns.

Proof. Indeed, the hypotheses (H_2) assert that the equilibrium (W_p^*, W_z^*) is stable for the system (2). For the system (7), the equilibrium becomes unstable if $\mathrm{Re}(\lambda \pm (\zeta))$ it passes from a negative value to a positive value checking with the following bifurcation parameters. Consider θ^p as a bifurcations parameter, the critical value of Turing is considered θ^p.

$$(\theta^p)_T = d_2 - u_2 + \frac{\delta_1 f_{W_p^*}^2}{2f_{W_z^*} + f_{W_p^*} + \sqrt{2f_{W_z^*} + f_{W_p^*})^2 - f_{W_p^*}^2 g_{W_z^*}^2}}$$

The w_T wavelength associated with the critical value $(\theta_p)_T$ is given by

$$w_T = \frac{2\pi}{k_T} = 2\pi\sqrt{\frac{2d_1\delta_T}{(\theta^p)_T + u_2 - d_2 + \delta_T f_{W_p^*}}},\ \ \delta_T = ((\theta^p)_T + d_2 - u_2)\,\frac{2f_{W_z^*} + f_{W_p^*} + \sqrt{2f_{W_z^*} + f_{W_p^*})^2 - f_{W_p^*}^2}}{f_{W_p^*}^2}.$$

The critical value of Hopf is

$$(\theta^p)_H = d_2 - u_2 + d_1\left[\frac{\gamma(1 - W_p^*)}{W_p^* + \gamma_1} + 2W_p^* - 1\right] \tag{33}$$

The region of instability Hopf is given by $\theta^p > (\theta^p)_H$ and the frequency of the oscillations is

$$\mu_H = \sqrt{\det(M)} = \sqrt{\left(\frac{(\theta^p)_H + u_2 - d_2}{d_1}\,\frac{1 - a - \gamma_1 - 2W_p^*}{W_p^* + \gamma_1}W_p^*\right)}.$$

The wavelength is

$$w_H = \frac{2\pi}{\mu_H} = \frac{2\pi}{\sqrt{\left(\frac{(\theta^p)_H + u_2 - d_2}{d_1}\,\frac{1 - a - \gamma_1 - 2W_p^*}{W_p^* + \gamma_1}W_p^*\right)}}.$$

4. Numerical Simulations

The following numerical simulations, carried out using the finite difference method, aim to study other behaviours of the dynamic system (7) under certain biologically reasonable parameters.

4.1. Numerical Scheme

At the origin $r = 0$, the equation (7) is not defined. In order to put ourselves in conditions of regularity and avoid singularity of scheme with finite differences [6], we use a uniform grid with a certain constant originally. This pole considers plays the role of a boundary condition which is an indispensable condition in the finite difference scheme. By discretization, the approximation of the problem (7) takes the form next:

We have for $n = 1...N$, with $N = \dfrac{T}{\triangle t}$ $i = 1...P + 1$ and $j = 1...M + 1$, we define $\{W_{p\,i,j}^{an}, W_{z_{i,j}}^{bn}\}$ such that

$$\begin{cases} \partial_n W_{p_{i,j}}^n = \triangle_{r_i\theta_j} W_{p_{i,j}}^n + f(\overrightarrow{W_{p_{i,j}}^n}, \overrightarrow{W_{z_{i,j}}^{(n-1)}}), \\ \partial_n W_{z_{i,j}}^n = \triangle_{r_i\theta_j} W_{z_{i,j}}^n + g(\overrightarrow{W_{p_{i,j}}^n}, \overrightarrow{W_{z_{i,j}}^{(n-1)}}), \end{cases} \tag{34}$$

where

$$\begin{cases} f(\overrightarrow{W^n_{p_{i,j}}}, \overrightarrow{W^{(n-1)}_{z_{i,j}}}) = r_p W^{(n-1)}_{p_{i,j}} - v_1 W^{(n-1)}_{p_{i,j}} \mid W^{(n-1)}_{p_{i,j}} \mid - \dfrac{u_1 \mid W^{(n-1)}_{p_{i,j}} \mid W^{(n-1)}_{z_{i,j}}}{\mid W^{(n-1)}_{p_{i,j}} \mid + e_1}, \\ g(\overrightarrow{W^n_{p_{i,j}}}, \overrightarrow{W^{(n-1)}_{z_{i,j}}}) = d_2 W^n_{z_{i,j}} - \theta^p W^{(n-1)}_{z_{i,j}} - u_e W^{(n-1)}_{z_{i,j}} - \dfrac{d_3 W^{(n-1)}_{z_{i,j}}}{\mid W^{(n-1)}_{p_{i,j}} \mid + e_2} W^{(n-1)}_{z_{i,j}}. \end{cases} \tag{35}$$

with $\overrightarrow{W^n_{p_{i,j}}} = (W^n_{p_{i,j}}, W^n_{z_{i,j}})^T$ denotes the two-dimensional approximation of the point (r_i, θ_j, t_n) with $t_n = n\Delta t$. The approximations of the initial conditions are given as follows: $W_{p_{i,j}}0 = W_p0(r_i, \theta_j)$, $W_{z_{i,j}}0 = W_z0(r_i, \theta_j)$. We choose a grid in the form

$$r_i = (i - \frac{1}{2})\Delta r, \;\; \theta_j = (j-1)\Delta\theta, \tag{36}$$

where $\Delta r = \dfrac{2}{2P+1}$, $\Delta\theta = \dfrac{2\pi}{M}$. Using the center difference method to discretize the Laplace operator, for $i = 2, ..., P$ and $j = 1, ..., M$ we have:

$$\Delta_{r_i\theta_j} W^n_{p_{i,j}} \approx \frac{W^n_{p_{i+1,j}} + W^n_{p_{i-1,j}} - 2W^n_{p_{i,j}}}{\triangle r^2} + \frac{W^n_{p_{i+1,j}} - W^n_{p_{i-1,j}}}{2r_i \triangle r} + \frac{W^n_{p_{i,j+1}} + W^n_{p_{i,j-1}} - 2W^n_{p_{i,j}}}{r_i^2 \triangle\theta^2}, \tag{37}$$

from the Neumann bounded conditions we have:

$$\frac{W^n_{p_{P+1,j}} - W^n_{p_{P,j}}}{\triangle r} = 0 = \frac{W^n_{z_{P+1,j}} - W^n_{z_{P,j}}}{\triangle r}, \tag{38}$$

so that the numerical limit values at $r = 1$, a $W^n_{p_{P+1,j}}$, can be approximated by a $W^n_{p_{P,j}}$ and $W^n_{p_{i,0}} = W^n_{p_{i,M}}$, $\quad W^n_{p_{i,1}} = W^n_{p_{i,M+1}}$ since W_p is 2π periodic in θ. For $i = 1$, the equation (37) is written

$$\Delta_{r_1\theta_j} W^n_{p_{1,j}} \approx \frac{W^n_{p_{2,j}} + W^n_{p_{0,j}} - 2W^n_{p_{1,j}}}{\triangle r^2} + \frac{W^n_{p_{2,j}} - W^n_{p_{0,j}}}{2r_1 \triangle r} + \frac{W^n_{p_{1,j+1}} + W^n_{p_{1,j-1}} - 2W^n_{p_{1,j}}}{r_1^2 \triangle\theta^2}, \tag{39}$$

since $r_1 = \dfrac{\Delta r}{2}$, the term $W^n_{p_{0,j}}$ is simplified and the equation (39) gives

$$\Delta_{r_1\theta_j} W^n_{p_{i,j}} \approx \frac{2(W^n_{p_{2,j}} - W^n_{p_{1,j}})}{\triangle r} + \frac{W^n_{p_{1,j+1}} + W^n_{p_{1,j-1}} - 2W^n_{p_{1,j}}}{r_1^2 \triangle\theta^2}, \tag{40}$$

It comes that

$$\begin{pmatrix} B_1 & 0 \\ 0 & B_2 \end{pmatrix} = \begin{pmatrix} \overrightarrow{w^n_p} \\ \overrightarrow{w^n_z} \end{pmatrix} = \begin{pmatrix} \overrightarrow{w^{n-1}_p} + \triangle t F \\ \overrightarrow{w^{n-1}_z} + \triangle t G \end{pmatrix}, \begin{pmatrix} B_1 = I + \triangle t L \\ B_2 = I + \delta \triangle t L \end{pmatrix}$$

I is the identity matrix and L is the matrix of coefficients in polar coordinates, F and G are associated with system (35).

$$A = \begin{pmatrix} -2 & 1+\mu_1 & 0 & ... & ... & 0 \\ 1-\mu_2 & \ddots & \ddots & \ddots & \ddots & \vdots \\ 0 & \ddots & \ddots & 1+\mu_i & \ddots & \vdots \\ \vdots & \ddots & 1-\mu_i & \ddots & \ddots & \vdots \\ \vdots & \ddots & \ddots & \ddots & -2 & 1+\mu_{P-1} \\ 0 & ... & ... & 0 & 1-\mu_P & 1+\mu_P \end{pmatrix}$$

$$D = \begin{pmatrix} \beta_1 & 0 & ... & ... & ... & 0 \\ 0 & \ddots & \ddots & \ddots & \ddots & \vdots \\ \vdots & \ddots & \beta_i & \ddots & \ddots & \vdots \\ \vdots & \ddots & \ddots & \ddots & \ddots & \ddots \\ \vdots & \ddots & \ddots & \ddots & \ddots & 0 \\ 0 & ... & ... & ... & 0 & \beta_p \end{pmatrix}$$

where

$$\beta_i = \frac{1}{(i-0.5)^2\Delta\theta^2}, \ \mu_i = \frac{1}{(i-0.5)}, \ i = 1, ..., P.$$

with

$$L = \begin{pmatrix} A-2D & D & 0 & ... & 0 & D \\ D & \ddots & \ddots & \ddots & \ddots & 0 \\ 0 & \ddots & \ddots & \ddots & \ddots & \vdots \\ \vdots & \ddots & \ddots & \ddots & \ddots & 0 \\ 0 & \ddots & \ddots & \ddots & \ddots & D \\ D & 0 & ... & 0 & D & A-2D \end{pmatrix},$$

4.2. Numerical Results

We can clearly see the determination of the analytic solution of our reaction diffusion system is not always possible. So, we solve the system (7) numerically, in order to present the spatial distribution over time and the effect of diffusion on training patterns on a circular domain. The Laplacian is computed using the finite element method. The numerical simulation observed different types of dynamics in the model studied. The blue color corresponds to a low population density and red one to a high density. The derivatives are approached by divergences on spatial Δx measures and the Euler method explicit for temporal integration with a size of time step Δt, such that the boundary conditions are of Neumann type. In order to avoid numerical artefacts, the value of time Δt and the spacing steps Δr and $\Delta\theta$ have been chosen sufficiently small, satisfying the criterion of CFL (Courant-Friedrichs-Levy) stability for the diffusion equation, [10]. We consider the following conditions:

$$\Delta t \leq \frac{r_i^2\Delta r^2\Delta\theta^2}{2r_i^2\Delta\theta^2 + r_i\Delta r\Delta\theta^2 + 2\Delta r^2}, \quad \text{for the system (7)1}$$

and

$$\Delta t \leq \frac{r_i^2\Delta r^2\Delta\theta^2}{\delta(2r_i^2\Delta\theta^2 + r_i\Delta r\Delta\theta^2 + 2\Delta r^2)}, \quad \text{for the system (7)2.}$$

The system is studied on a spatial domain $\Omega = \left\{(x,y) \in \mathbb{R}^2 : x^2 + y^2 < 500\right\}$. The simulation environment used is the Matlab software. The initial condition is a small disturbance of the W^* equilibrium point as follows:

$$W_{p,0}(r_i,\theta_j) = W_p^*((r_i cos\theta_j)^2 + (r_i sin\theta_j)^2) = W_p^* r_i^2 < 500,$$

$$W_{z,0}(r_i,\theta_j) = W_z^*((r_i cos\theta_j)^2 + (r_i sin\theta_j)^2) = W_z^* r_i^2 < 500.$$

The values of the parameters used for the numerical simulation are in Table 1.

Table 1. *Parameters values used for the numerical simulation.*

Parameters	Values	References
v_0	0.01	[2, 13]
e_1	0.7	[3, 10]
e_2	0.1	[2, 3]
d_1	0.6	[4, 10]
d_2	0.6	[3, 4]
u_1	0.6	[12, 15]
d_3	0.002	[10, 13]
s_2	0.5	[4, 13]
s_1	1.5	[8, 15]

4.2.1. Bifurcation Diagram for the ODE Model

In Figure 2, we plot the curves of phytoplankton and zooplankton densities as a function of time t describing in the system (2) when the bifurcation parameter θ^p varies. All values of the parameters used are given in Table 1. For

$$\theta^p = 0.375 < (\theta^p)_T = 0.584,$$

we observe from Figure $2(A1, B1)$ and Figure $2(A2, B2)$ that the phytoplankton and zooplankton populations converge towards their stable states $E^* = (W_p^*, W_z^*)$. Figure $2(A2, B2)$ shows the stability of those populations. The existence of centers (Figures 2 (B2)) confirms the coexistence of these two species for some toxin value released by phytoplankton. For

$$\theta^p = 0.637 > (\theta^p)_T = 0.584,$$

we have a first bifurcation. The equilibrium point $E^* = (W_p^*, W_z^*)$ loses its stability and becomes unstable in Figure $3(A3, B3)$ and we have a presence of limit cycle. If we increase the value of

$$\theta^p = 0.9248 > (\theta^p)_T = 0.584,$$

the system stays unstable (see Figure $3(A4, B4)$) and we have a limit cycle. The simulations make us suppose that the solution is bounded for any positive initial conditions $W_{p_0} = 2.75$ and $W_{z_0} = 8.25$. These results corroborate with the results of stability obtained in proposition 3.7 and theorem 3.2.

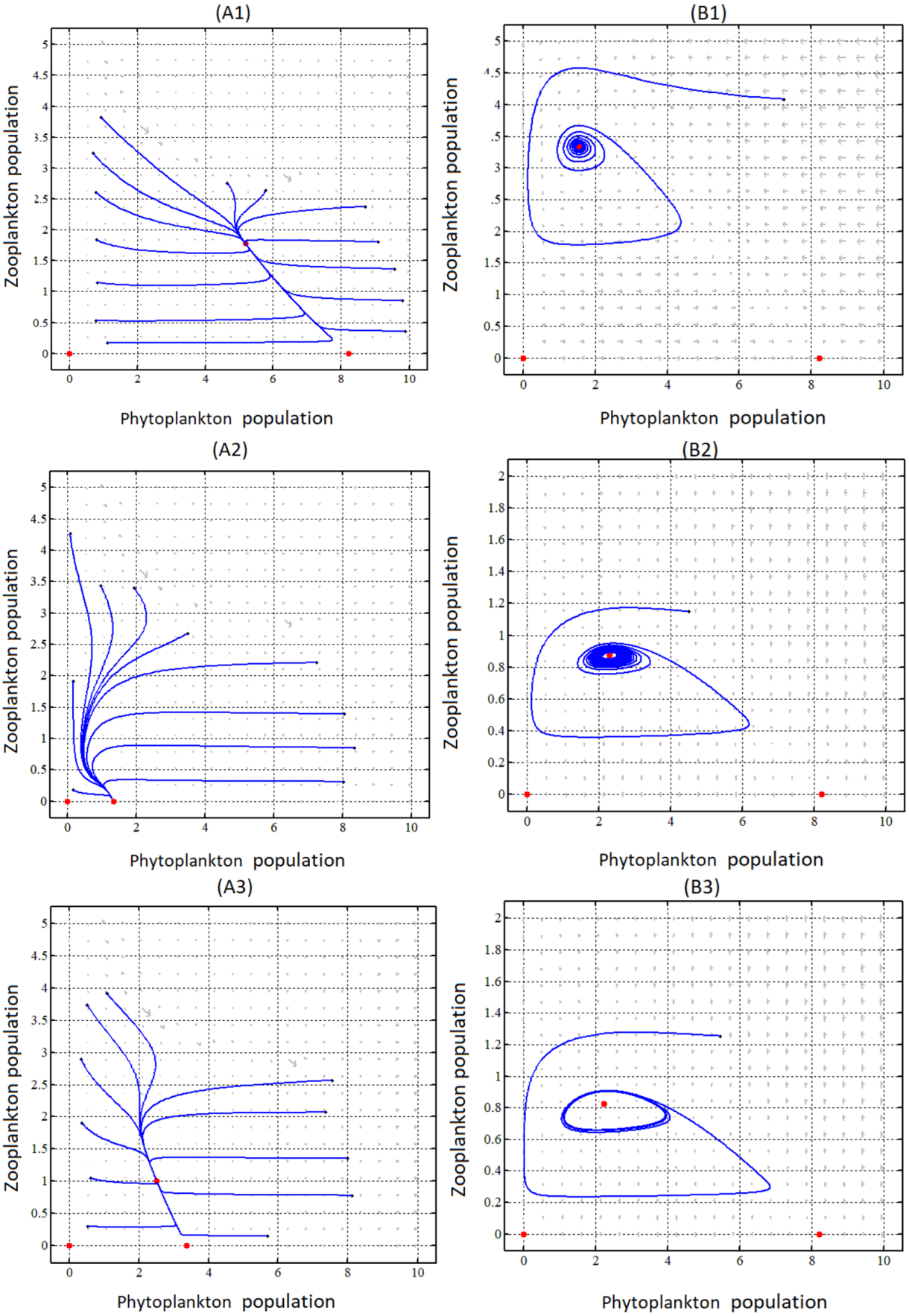

Figure 2. *Locally asymptotic stability of the coexisting positive equilibrium of the system phytoplankton-zooplankton with* $\theta^p = 0.375 < (\theta^p)_T = 0.584$. *The influence of varying the parameter* θ^p *on the system's* (2)*dynamic is explained in the phase plane* (H_p, H_z). *Consequently of proposition 3.2, the total populations are uniformly weakly persistent and the solution will either converge to* E^*.

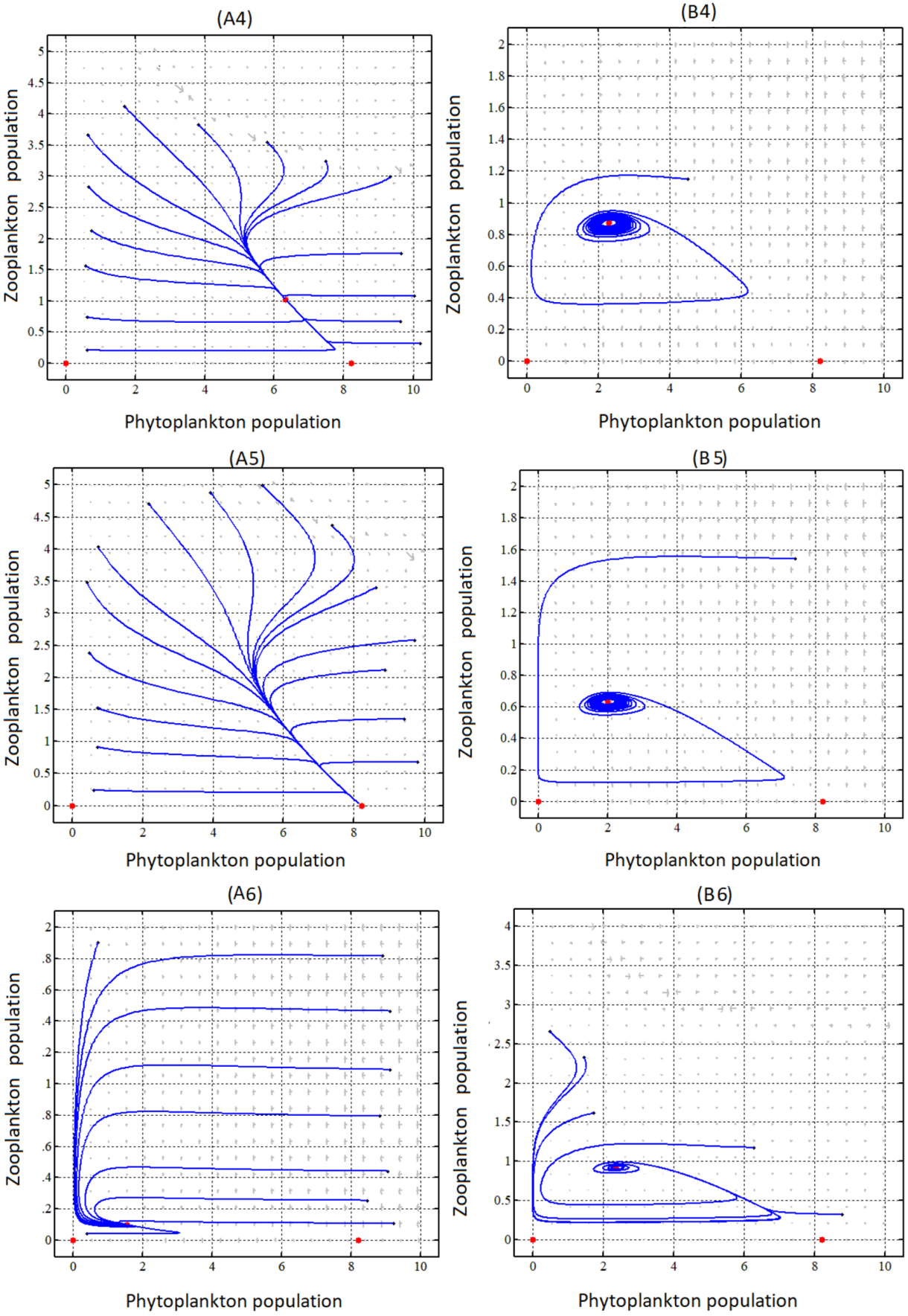

Figure 3. *Locally asymptotic stability of the coexisting positive equilibrium of the system phytoplankton-zooplankton with* $\theta^p = 0.637 > (\theta^p)_T = 0.584$ *in figure* $3(A3, B3)$, $3(A4, B4)$*and* $\theta^p = 0.9248 > (\theta^p)_T = 0.584$ *in figure* $3(A5, B5)$ *and* $3(A6, B6)$. *The influence of varying the parameter* θ^p *on the system's* (2) *dynamic is explained in the phase plane* (P, Z). *Consequently of proposition 3.1, the total populations are uniformly weakly persistent and the solution will either converge to a periodic function in the two cases (see figure 3).*

4.2.2. Pattern Formation of the PDE Model

We consider that the value of released toxin is $\theta^p = 0.07$ and the two species diffuse in the same way i.e. $\delta_0 = \delta_1$. Numerical simulations show that after a transitional phase, we notice the formation of patterns throughout the field. First, in Figure 4, we observe a spiral-wave type spatial distribution for the system (7). Figure 4 shows the evolution of the spatial distribution of species. The Figures on the left are the evolution of the spatial distribution of the phytoplankton and that on the right of the zooplankton. We first observe two spot-shaped waves that form Figure 4 at $(A_1, B_1) - (A_8, B_8)$ with $\delta_0 = \delta_1 = 0.9$. Then, these spots explode leading to an aperiodic spatial distribution on a part of the domain. Then, this aperiodicity spreads over the entire domain and leads to the formation of the patterned bands over the entire domain (see figure 4) with $4(A_7, B_7), T = 8000$ and $4(A_8, B_8), T = 10000$. The different time is used in others figure as follows:

Table 2. *The first times values used for the numerical simulation for $\theta^p = 0.07$.*

Figs	$4(A_1, B_1)$	$4(A_2, B_2)$	$4(A_3, B_3)$	$4(A_4, B_4)$
Time	300	500	1000	4000

Table 3. *The second times values used for the numerical simulation for $\theta^p = 0.07$.*

Figs	$4(A_5, B_5)$	$4(A_6, B_6)$
Time	5000	6000

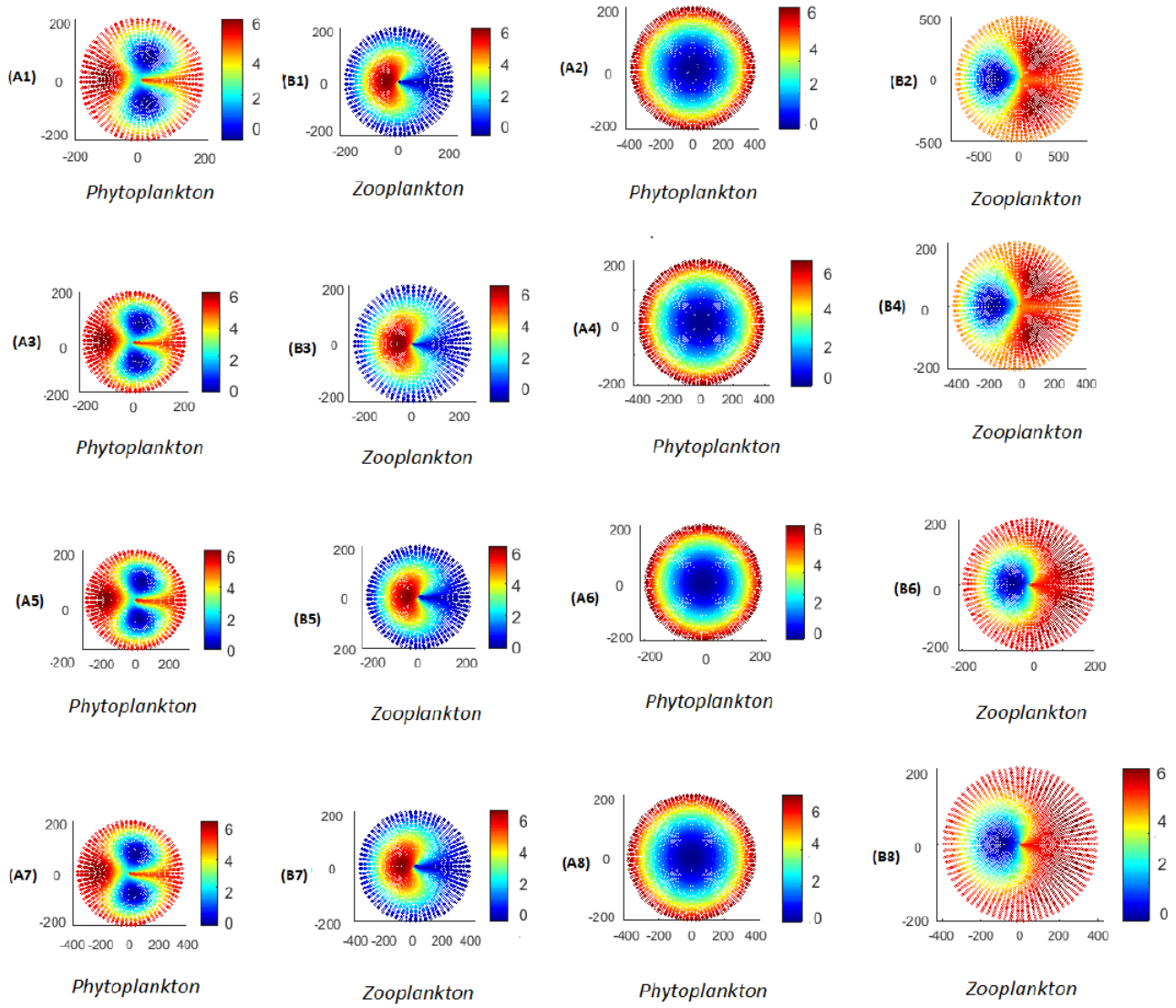

Figure 4. *Spiral wave type spatial distribution for $\delta_0 = \delta_1 = 0.9$. we have plotted a different view of snapshots of species W_p (W_z follows a similar evolution), where both figures use the same color scale. We readily see that for spatial patterns, their amplitude does not varies in time.*

In the second time, in Figure 5, we observe a spiral-wave type spatial distribution for the system (7). Figure 5 shows the evolution of the spatial distribution of species. The Figures on the left are the evolution of the spatial distribution of the phytoplankton and that on the right of the zooplankton. We first observe two spot-shaped waves that form Figure 5 at $(A_1, B_1) - (A_{10}, B_{10})$ with $\delta_0 = \delta_1 = 0.5$. Then, these spots explode leading to an aperiodic spatial distribution on a part of the domain. Then, this aperiodicity spreads over the entire domain and leads to the formation of the patterned bands over the entire domain (see Figure 5). The different time is used as follows and $T = 30000$ at Figure $5(A_7, B_7)$, $T = 50000$ at Figure $5(A_8, B_8)$, $T = 52000$ at Figure $5(A_9, B_9)$,$T = 55000$ at Figure $5(A_{10}, B_{10})$:

Table 4. *The first times values used for the spiral-wave type spatial distribution.*

Figs	$\mathbf{5(A_1, B_1)}$	$\mathbf{5(A_2, B_2)}$	$\mathbf{5(A_3, B_3)}$	$\mathbf{5(A_4, B_4)}$
Time	5000	8000	10000	15000

Table 5. *The second times values used for the spiral-wave type spatial distribution.*

Figs	$\mathbf{5(A_5, B_5)}$	$\mathbf{5(A_6, B_6)}$
Time	20000	22000

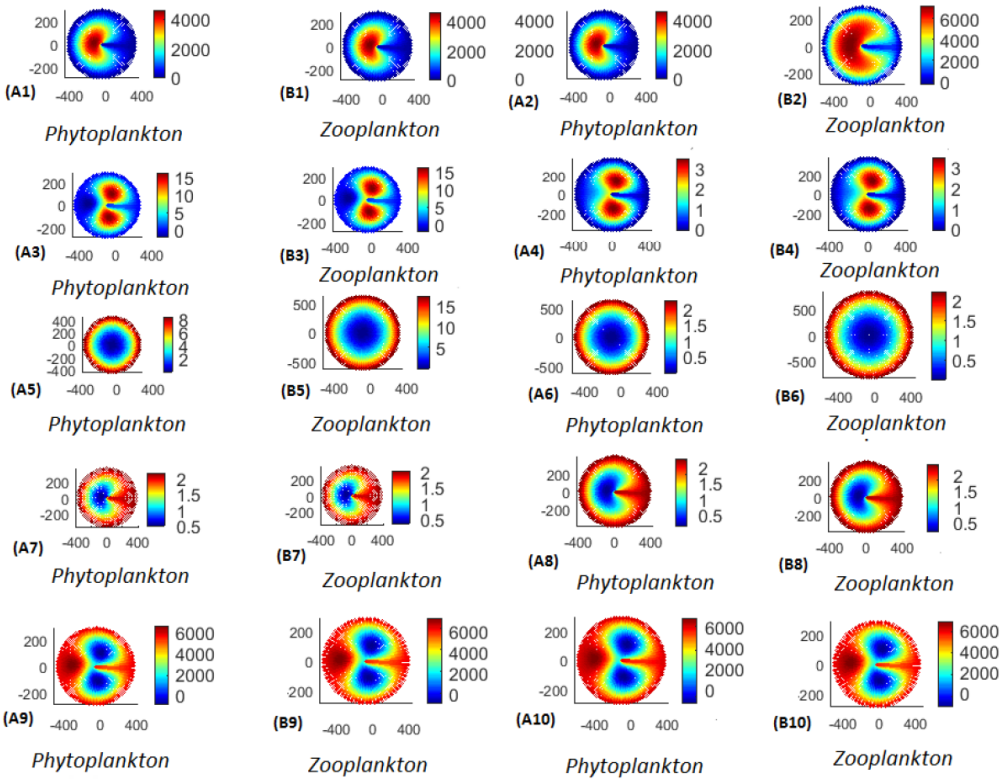

Figure 5. *Spatial distribution of species for $\delta_0 = \delta_1 = 0.5$ we have plotted a different view of snapshots of species W_p (W_z follows a similar evolution), where both figures use the same color scale. We readily see that for spatial patterns, their amplitude does not varies in time.*

4.3. Analysis of the Dynamics Behaviour with Toxin Effect

We continue the numerical study to examine the behaviour of the dynamics of the system (7) considering different values of the toxin. We consider $\delta_0 = 0.9$, $\delta_1 = 0.9$ and using $T = 12000$. The different values of toxin released is used as follows $\theta^p = 0.86$ at Figure $6(A_7, B_7)$, $\theta^p = 0.9248$ at Figure $6(A_8, B_8)$:

Table 6. *The first θ^p values used for the spatial distribution.*

Figs	$\mathbf{6(A_1, B_1)}$	$\mathbf{6(A_2, B_2)}$	$\mathbf{6(A_3, B_3)}$	$\mathbf{6(A_4, B_4)}$
Time	0.12	0.37	0.41	0.584

Table 7. *The second θ^p values used for the spatial distribution.*

Figs	$\mathbf{6(A_5, B_5)}$	$\mathbf{6(A_6, B_6)}$
Time	0.60	0.79

Numerical results show that the release of the toxin can induce distribution patterns space that can be useful in understanding the complex dynamics of ecosystems sailors. Figure 6 shows the behaviour of both zooplankton and phytoplankton populations. In Figure 6, the cases $(A_1, B_1) - (A_4, B_4)$ show how stability can be achieved the dynamics if the toxin is released with $\theta^p \in (0.12, 0.9248)$. However, for the case $(A_5, B_5) - (A_8, B_8)$ find, a more dense distribution

of the phytoplankton population compared to zooplankton and this confirms the effect of the toxin on the behaviour of population dynamics of zooplankton.

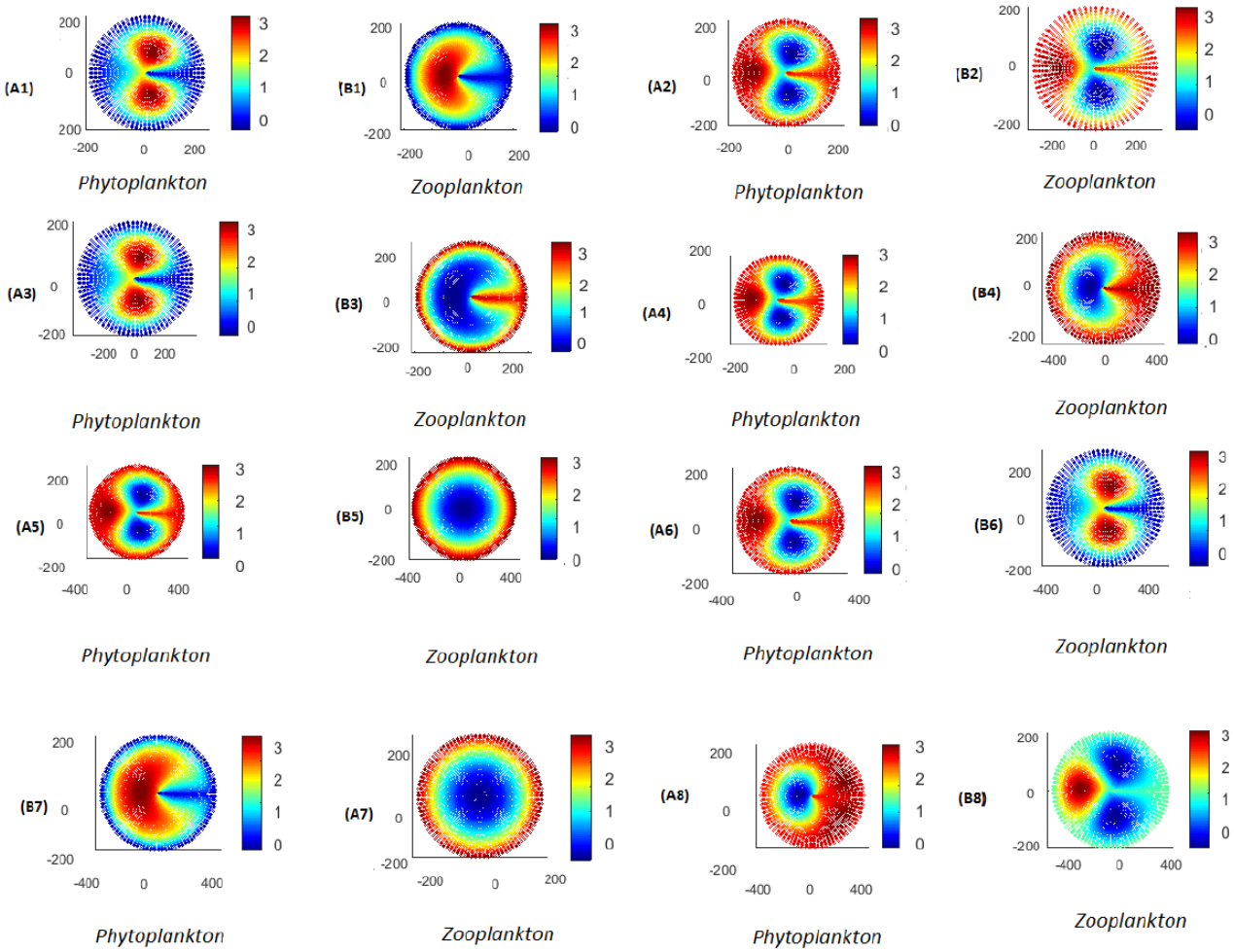

Figure 6. *Spatial distribution with diffusion for phytoplankton and zooplankton populations. Spatial behaviour are obtained with coefficients of diffusion at* $T = 12000$. *The spatial distribution is obtained with different values of the toxin:* $\theta_p = 0.12(A_1, B_1), \theta^p = 0.37 - (A_2, B_2)$; $\theta^p = 0.41(A_3, B_3)$; $\theta^p = 0.584(A_4, B_4), \theta^p = 0.60(A_5, B_5), \theta^p = 0.79(A_6, B_6)$; $\theta^p = 0.86(A_7, B_7)$; $\theta^p = 0.9248(A_8, B_8)$.

Remark 4.1. The period $(\theta^p > (\theta^p)_T = 0.584)$ corresponds to the proliferation of phytoplankton. Here, these observations indicate us that to maintain the operating order of an ecosystem, we have to control the toxin releasing on the domain.

4.4. Conclusion

In recent years, many scientific results have been able to easily show the role played by phytoplankton in controlling blooms or reducing grazing pressure in the aquatic environment. But the functional mechanisms used by phytoplankton to release the toxic substance are not sufficiently known [4, 12]. It is in this perspective that in this article, we considered a form of diffusion to describe the population of zooplankton and phytoplankton on a circular domain, taking into account a toxin control parameter. The construction of the model is derived from an nonlinear ODE system approaching the principle of modelling as the works of Holling, [3, 4, 10]. Assumptions are made on the independence of diffusion and spatial variables for the formulation of this modified nonlinear systems of reaction-diffusion type model approach with a Holling II type functional response. We use the mathematical technical tools based specifically on the analytical technique. The The mathematical analysis made it possible to bring out equilibrium existence conditions that depend on demographic parameters. We also gave some results on the stability of the equilibria of the ODE and PDE systems. We have described the conditions to give the Turing patterns and the critical values of the Turing and Hopf bifurcation under certain conditions concerning the toxin parameters. The above results indicate that the strength of the toxic substances released by phytoplankton reduces the prevalence of chaos. We manage to control during our simulations that for $\theta^p > (\theta^p)_T = 0.584$ the effect of the toxin produced by phytoplankton

becomes detrimental to the dynamics of the zooplankton-phytoplankton system in the environment. The conclusion of such observation is that the functional form of release of toxic substances by the phytoplankton population can act as control by changing the state of chaos into a state of order [8, 13, 15]. Since the aquatic systems being very complex, especially on a circular domain, it is sometimes difficult to conclude that the order of operation in aquatic ecosystem is obvious, especially on a circular domain. The importance of the population of the phytoplankton in the aquatic ecosystem as for the clear mechanism of the release of the toxin is still in its infancy. The practical development of this subject requires a particular concentration on the part of the experimental and mathematical ecologists. With this work developed in this article, we are convinced to have brought some insights in this direction. Phytoplankton blooms were observed in our simulations and are in agreement with biological observations.

Despite the important results on the study of this dynamics, in order to deepen our results, we plan, for our future work, to consider differently the toxic environment composed of different populations of phytoplankton which do not compose the toxin and those which are toxic in order to finally extend to better control of the global mode of operation of toxin on a circular aquatic domain.

ORCID

0009-0004-2256-4154 (Hamidou Ouedraogo)
0009-0001-4129-037X (Wendkouni Ouedraogo)
0009-0001-7514-3052 (Desire Ouedraogo)
0000-0002-9780-4966 (Boureima Sangare)

Authors Contributions

Hamidou Ouedraogo: Conceptualization, Formal Analysis, Investigation, Methodology, Software, Supervision, Validation, Visualization, Writing - original draft, Writing - review & editing

Wendkouni Ouedraogo: Conceptualization, Data curation, Formal Analysis, Investigation, Methodology, Software, Supervision, Validation, Visualization, Writing - original draft, Writing - review & editing

Desire Ouedraogo: Formal Analysis, Validation, Visualization, Writing - original draft, Writing - review & editing

Boureima Sangare: Conceptualization, Data curation, Formal Analysis, Supervision, Validation, Visualization, Writing - original draft, Writing - review & editing

Funding

This paper is not funded.

Conflicts of Interest

The authors declare no conflicts of interest.

References

[1] W. Abid, Analyse de la Dynamique de Certains Modeles Proie-Predateur et Applications, These de doctorat de Mathematiques, *Universite du Havre*, French, 2016.

[2] V. Ajraldi, M. Pittavino, E. Venturino, Modeling herd behavior in population systems, *Nonlinear Anal. Real World Appl.* 12 vol 4: pp. 2319-2338, 2011, https://doi.org/10.1016/j.nonrwa.2011.02.002

[3] M. Aziz-Alaoui, M. Daher Okiye, Boundedness and global stability for a predator-prey model with modified Leslie-Gower and Holling type II shemes, *Appl. Math. Letter.* 7 vol 16: pp. 1069-1075, 2003, https://doi.org/10.1016/S0893-9659(03)90096-6

[4] M. Banerjee and E. Venturino, A phytoplankton-toxic phytoplankton-zooplankton model *Ecol. Complex.,* vol 8: pp. 239-248, 2011, https://doi.org/10.1016/j.ecocom.2011.04.001

[5] S. Chakraborty, S. Chatterjee, E. Venturino and J. Chattopadhyay, Recurring plankton bloom dynamics modeled via toxin-producing phytoplankton, *J. Biol. Phys.* vol 3: pp. 271-290, 2008, https://doi.org/10.1007/s10867-008-9066-3

[6] G. Galiano, M. L. Garzon, A. Jungel, Semi-discretization in time and numerical convergence of solutions of a nonlinear cross-diffusion population model, *Numer. Math.* 4 vol 93: pp. 655-673, 2003, http://nbn-resolving.de/urn:nbn:de:bsz:352-opus-21507

[7] Y. F. Lv, Y. Z. Pei, S. J. Gao, & C. G. Li, (2010). Harvesting of a phytoplankton-zooplankton model. *Nonlinear Analysis*, vol. 11, no. 5, pp. 3608-3619, https://doi.org/10.1016/j.nonrwa.2010.01.007

[8] M. R. May, Chaos in natural populations, *Proc. Roy. Soc.,* A 27: pp 419-428. 19, 1987, https://link.springer.com/chapter/10.1007/978-0-85729-115-824

[9] M. M. Mullin, E. F. Stewart and F. J. Fuglister, Ingestion by planktonic grazers as a function of concentration of food1 *Limnol. Oceanogr.* vol 20: pp. 259-262, 1975, https://doi.org/10.4319/lo.1975.20.2.0259

[10] H. Ouedraogo, W. Ouedraogo, B. Sangaré, Bifurcation and stability Analysis in Complex Cross-Diffusion Mathematical Model of Phytoplankton-Fish Dynamics *J. Part. Diff. Eq.* 3 vol 32: pp. 207-228, 2019, https://doi.org/10.4208/jpde.v32.n3.2

[11] R. Pal, D. Basu and M. Banerjee, Modelling of phytoplankton allelopathy with Monod-Haldane-type functional response-A mathematical study *Biosystems.* vol 95: pp. 243-253, 2009, https://doi.org/10.1016/j.biosystems.2008.11.002

[12] Rao F. (2013). Spatiotemporal dynamics in a reaction-diffusion toxic-phytoplankton-zooplankton model. *Journal of Statistical Mechanics: Theory and Experiment.* vol. 2013, pp. 114-124, https://doi.org/10.1016/j.rico.2024.100478

[13] R. K. Upadhyay, S. R. K. Iyengar, V. Rai. Chaos: An ecological reality, *Int. J. Bifur. Chao.* 8(6), pp. 1325-1333, 1998, https://doi.org/10.1142/S0218127498001017

[14] S, Yao, J. Yang and S. Yuan, Bifurcation analysis in a modified Leslie-Gower predator-prey model with fear effect and multiple delays, *Mathematical Biosciences and Engineering.* 4 vol 21. 5658-5685, 2024, https://doi.org/10.3934/mbe.2024249

[15] S. ZHAO, P. YU, AND H. WANG, Spatiotemporal Patterns in a Lengyel-Epstein Model Near a Turing-Hopf Singular Point, Siam J. Appl. Mat., 2 vol 84, pp 338-361, 2024, https://doi.org/10.1137/23M1552668